Control Engineering Practice 45 (2015) 230–243

Contents lists available at ScienceDirect

Control Engineering Practice

journal homepage: www.elsevier.com/locate/conengprac

On the dynamics and control of flexible joint space manipulators

Kostas Nanos, Evangelos G. Papadopoulos *

School of Mechanical Engineering, National Technical University of Athens (NTUA), 9 Heroon Polytechneiou street, 15780 Athens, Greece

ARTICLE INFO

Article history:
Received 30 May 2014
Received in revised form
27 March 2015
Accepted 26 June 2015
Available online 5 August 2015

Keywords:
Space robots
Flexible joints
Dynamics
Control

ABSTRACT

Space manipulator systems are designed to have lightweight structure and long arms in order to achieve reduction of fuel consumption and large reachable workspaces, respectively. Such systems are subject to link flexibilities. Moreover, space manipulator actuators are usually driven by harmonic gear mechanisms which lead to joint flexibility. These types of flexibility may cause vibrations both in the manipulator and the spacecraft making the positioning of the end-effector very difficult. Here, both types of flexibilities are lumped at the joints and the dynamic equations of a general flexible joint space manipulator are derived. Their internal structure is highlighted and similarities and differences with fixed-base robots are discussed. It is shown that one can exploit the derived dynamic structure in order to design a static feedback linearization control law and obtain an exact linearization and decoupling result. The application of such controllers is desired in space applications due to their small computational effort. In case of fixed-base manipulators, the effective use of a static feedback controller is feasible only if a simplified model is considered. Then, the proposed static feedback linearization control law is applied to achieve end-effector precise trajectory tracking in Cartesian space maintaining a desirable non-oscillatory motion of the spacecraft. The application of the proposed controller is illustrated by a planar seven degrees of freedom (dof) system.

1. Introduction

In space applications, manipulator construction is different than that in terrestrial manipulators. To reduce launch mass and increase workspace, the design of lightweight and long reach manipulators is strongly preferred. However, a problem of such lightweight space manipulators is the increased structural flexibility of the links. This link flexibility causes structural vibrations, which are profound when manipulating large payloads. In addition to link flexibilities, space manipulators are also subject to joint flexibilities. Such flexibilities arise primarily due to motor torque ripples, joint transmission elements such as gears (e.g., harmonic drives), and actuator shafts.

In this paper, all system flexibilities are lumped to joint flexibilities, aiming in studying their effects in the design of control systems, and in endpoint positioning. Lumping of all flexibilities at the joint level is reasonable for systems with short links, such as the free-floating/free-flying space manipulator systems under study, or for flown systems such as the ETS-7 and the Orbital Express.

The control of flexible joint space robotic manipulators represents a very challenging problem, mainly because the number of degrees of freedom of the system is twice as the number of control inputs. In some cases, joint flexibility can lead to instability, when neglected in the control design.

In most papers, the flexibility of the robot structure is neglected. This assumption is acceptable if the robot structure is stiff enough. In space applications where lightweight structures are desired, the avoidance of flexibility effects requires very slow motions of the manipulator. However, manipulator oscillations may become evident even in very slow motions when very large payloads are handled.

Over the past decades, dynamic models of different detail level have been proposed for fixed-base manipulators with flexible joints. A simplified model, the so called *reduced* model assumes that the angular kinetic energy of the rotors of the motors is due only to their relative spinning around the driving axes (Hung and Spong, 1989). A more accurate dynamic model, called *complete*, includes also the inertial couplings existing between the motors and the links (De Luca, 1998). Each of these models has different structural properties from the point of view of control.

Several controllers have been proposed to address the flexible joint control problem for fixed-base manipulators, including techniques similar to those for rigid robots. Tomei proposes a simple PD regulator for flexible joint robots, providing simulation results for a regulation problem about a reference position (Tomei, 1991). An extension of the PD regulator for flexible joint robot

* Corresponding author.
E-mail addresses: knanos@mail.ntua.gr (K. Nanos), egpapado@central.ntua.gr (E.G. Papadopoulos).

http://dx.doi.org/10.1016/j.conengprac.2015.06.009
0967-0661/

manipulators considering also actuators dynamics as well as friction is presented by Lozano, Valera, Albetos, Arimoto, and Nakayama (1999).

A different modelling approach called singular perturbation method can be applied when the joint stiffness is relatively large, but still finite. Then, the system exhibits a two-time scale dynamic behaviour in terms of rigid and elastic variables. Using this method, one can apply controllers which consist of a slow control action designed on the basis of a rigid robot model and a fast control action designed to damp the elastic oscillations at the joints (Hung & Spong, 1989).

As mentioned above, the model structure of fixed-base manipulators with elastic joints affects the control method. The reduced model can be fully decoupled and linearized exactly by means of a nonlinear *static state feedback control law*, similarly to the well-known computed torque method for rigid manipulators (Spong, 1987). On the other hand, when considering the more complete dynamics, a satisfactory end-effector control is feasible only by applying a more complex *dynamic state feedback controller* (De Luca and Lucibello, 1998). The application of these controllers, assume the availability of both motor and link angular position and velocity as well. However, the full state measurement of the elastic joint manipulator is not usually available. In such a case, the application of observer techniques is necessary. A new observer which uses only motor position sensing, together with accelerometers suitably mounted on the links of the robot arm was introduced by De Luca, Lucibello, Schroder, and Thummel (2007). Its main advantage is that the error dynamics on the estimated state is independent from the dynamic parameters of the robot links, and can be tuned with standard decentralized linear techniques.

It is well known that the manipulator natural frequencies are continuously changing with manipulator configuration and payload (Book, 1993). Moreover, in space applications, when handling large payloads, manipulator joint or structural flexibility becomes important and can result in payload-attitude controller fuel-replenishing dynamic interactions. Such interactions may lead to control system instabilities, or manifest themselves as limit cycles (Martin, Papadopoulod, & Angeles, 1999). Therefore, the control of these systems is more sophisticated.

Martin, Papadopoulos and Angeles examined the possible dynamic interactions between the attitude controller of a spacecraft and the flexible modes of a space manipulator mounted on it (Martin et al., 1999). The authors proposed a control scheme based on on–off thrusters valves, since proportional thruster valves and thus, classical PD and PID control laws were not initially in use. Hu and Vukovich applied the singular perturbation theory in order to control the object position and internal forces as well as the joint elastic forces for a free-flying space robotic system (Hu & Vucovich, 1997). However, the proposed controller does not guarantee a non-oscillatory motion of the manipulators and their spacecraft. Ferretti et al. proposed a torque controller for a two-mass system with elastic behaviour (Ferretti, Magnani, Rocco, Viganò & Rusconi, 2005). The results show that the use of the torque sensor in the joints of the DEXARM space robot would be beneficial for the purpose of high performance motion control. More recently, Ulrich and Sasiadek addressed the problem of adaptive trajectory control of space manipulators that exhibit elastic vibrations in their joints and that are subject to parametric uncertainties and modelling errors (Ulrich & Sasiadek, 2012). In order to control the space manipulator, an inertially-stabilized platform assumption was adopted.

In this paper, we study the dynamics of space manipulators, considering all the flexibilities lumped at the joints. In terrestrial manipulators a static feedback controller, with small computational effort, can be used only if a reduced model is considered. However the reduced model is not a realistic one in most cases since it assumes that the kinetic energy of each rotor is due only to its own rotation. If a complete model is considered, then a dynamic feedback controller should be applied increasing the computational effort. Note that the computational effort is an important factor in space applications. However, using the Lagrange approach, it is shown that the structure of the dynamics of the flexible joint space manipulators differs than the model structure of the terrestrial ones. Thus, the derived model structure gives new opportunities in the design of trajectory following controllers. Therefore, exploiting the structure of the derived dynamic model, the system can be linearized and decoupled via a static feedback linearization controller reducing the computational effort. Next, the proposed controller is applied so that the end-effector follows a desired path in Cartesian space in the presence of joint flexibilities maintaining a desirable non-oscillatory motion of the spacecraft. The application of the method is illustrated by an example.

2. Dynamics of flexible joint space manipulators

This section develops the dynamic equations of a flexible joint space manipulator. We consider a system whose manipulator has revolute joints and an anthropomorphic open chain kinematic configuration for maximum reachable workspace. Under the assumption of no external forces, the system Center of Mass (CM) does not accelerate, and the system linear momentum is constant. With the further assumption of zero initial linear momentum, the system CM remains fixed in inertial space, and the origin, O, can be chosen to be the system CM, see Fig. 1.

The N joints are actuated by DC brushless motors equipped with harmonic drive mechanisms. Due to the use of the harmonic drives, all joints are considered to be flexible. When reduction gears are present, they are modelled as being placed before the joint deflection occurs, see Fig. 2.

The dynamic model of flexible manipulators requires doubling of the generalized coordinates in a Lagrangian approach, i.e. both the link and gear reduction angular position $\mathbf{q}$ and $\boldsymbol{\theta}_\mathbf{m}$, respectively. The model derivation is accomplished using the following assumptions. (i) We consider small joint deflections. Thus, the elastic and dynamic friction effects of the harmonic drive mechanism are modelled using a torsion spring of constant stiffness k and a damping element b, respectively, as shown in Fig. 2. (ii) The actuator rotors are modelled as additional rigid bodies and having their CM on the rotation axis. The motor stators are considered to be mounted on manipulator links. (iii) Since the location of the

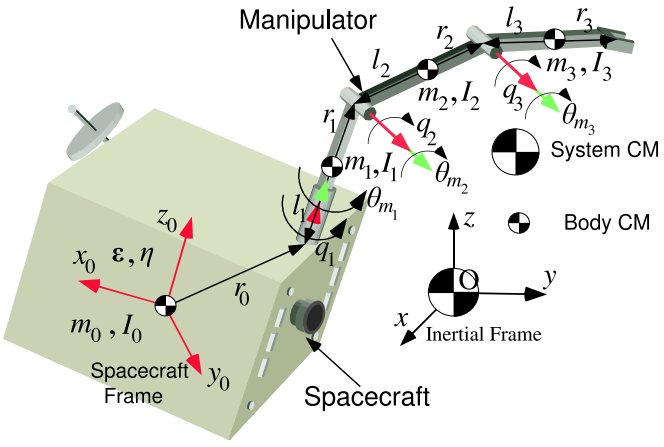

Fig. 1. A space robotic manipulator system.

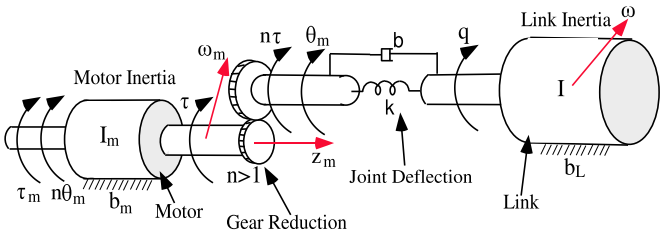

Fig. 2. The flexible joint model.

actuators along the manipulator structure has a great influence on the form of the derived equations of motion, we consider, for simplicity, that the i-th motor moves link i and is mounted on link $i-1$ with its rotation axis aligned with the i-th joint.

Next, we study the influence of the motors in the equations of angular momentum and the kinetic energy. The derivation of the equations of motion follows.

2.1. Motor effect on the system angular momentum

In free-floating mode, where the spacecraft actuators are turned-off and the control of the space system is feasible using only manipulator actuators, the conservation of the system angular momentum defines the spacecraft response according to the manipulator motion. Thus, first, we study the effect of motor inertia properties (mass and moment of inertia) on the system's angular momentum.

Consider the space manipulator link i and rotor i at joint i as shown in Fig. 3. The link has mass m_i and moment of inertia relative to its CM equal to $\mathbf{I_i}$. The rotor i has mass m_{mi} and $\mathbf{I_{mi}}$ is the moment of inertia with respect to its axis. The positions of the link and rotor CM from the space manipulator CM are at the distances $\boldsymbol{\rho_i}$ and $\boldsymbol{\rho_{mi}}$, respectively, see Fig. 3. The link angular velocity is $\boldsymbol{\omega_i}$ and the rotor's one is $\boldsymbol{\omega_{mi}}$, see Fig. 2.

The angular momentum of a N link space manipulator with respect to its CM, $\mathbf{h_{CM}}$, is given by

$$\mathbf{h_{CM}} = \mathbf{I_0}\cdot\boldsymbol{\omega_0} + m_0\boldsymbol{\rho_0}\times\dot{\boldsymbol{\rho}}_0 + \sum_{k=1}^{N}\left(\mathbf{I_k}\cdot\boldsymbol{\omega_k} + m_k\boldsymbol{\rho_k}\times\dot{\boldsymbol{\rho}}_k + \mathbf{I_{mk}}\cdot\boldsymbol{\omega_{mk}} + m_{mk}\boldsymbol{\rho_{mk}}\times\dot{\boldsymbol{\rho}}_{mk}\right) \tag{1}$$

where the index 0 corresponds to the spacecraft.

The angular velocity of the rotor k is given by

$$\boldsymbol{\omega_{mk}} = \boldsymbol{\omega_{k-1}} + n_k\dot{\theta}_{mk}\mathbf{z_{mk}} \tag{2}$$

where $n_k > 1$ is the reduction ratio at the i-th joint, θ_{mk} is the gear reduction angular position, see Fig. 2, $\mathbf{z_{mk}}$ is the unit vector in the direction of the rotor rotation axis and $\boldsymbol{\omega_{k-1}}$ is the angular velocity of the link $i-1$.

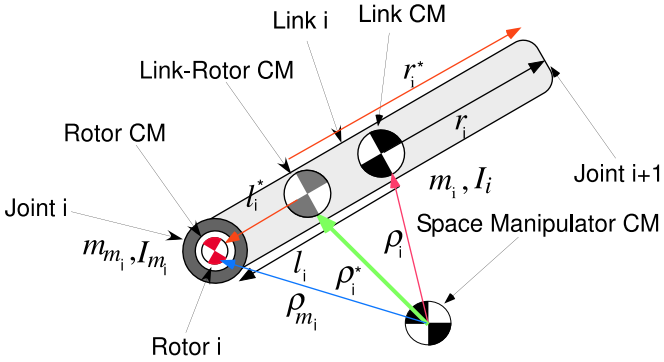

Fig. 3. Definition of the link-motor system CM.

The presence of the rotor shifts the CM of the system link-rotor at a new position given by the vector $\boldsymbol{\rho_i^*}$, see Fig. 3. The vectors $\mathbf{r_i^*}$ and $\mathbf{l_i^*}$ of the rotor-link CM from the link joints are shown in Fig. 3. Since the vectors $\boldsymbol{\rho_i^*}$, $\boldsymbol{\rho_i}$ and $\boldsymbol{\rho_{mi}}$ are defined with respect to the system CM, it can be shown that

$$\mathbf{r_i^*} = \mathbf{r_i} - \frac{m_{mi}}{m_i + m_{mi}}\mathbf{l_i} \tag{3a}$$

and

$$\mathbf{l_i^*} = \frac{m_i}{m_i + m_{mi}}\mathbf{l_i} \tag{3b}$$

where $\mathbf{r_i}$ and $\mathbf{l_i}$ are the corresponding vectors from the link CM, see Fig. 3.

Eq. (1) can be simplified, if one expresses the vectors $\boldsymbol{\rho_i}$ and $\boldsymbol{\rho_{mi}}$ as a function of the vector $\boldsymbol{\rho_i^*}$. It can be shown that

$$\boldsymbol{\rho_i} = \boldsymbol{\rho_i^*} - \frac{m_{mi}}{m_i + m_{mi}}\mathbf{l_i} \tag{4a}$$

and

$$\boldsymbol{\rho_{mi}} = \boldsymbol{\rho_i^*} + \frac{m_i}{m_i + m_{mi}}\mathbf{l_i} \tag{4b}$$

The time derivatives of the above vectors are as follows:

$$\dot{\boldsymbol{\rho}}_i = \dot{\boldsymbol{\rho}}_i^* - \frac{m_{mi}}{m_i + m_{mi}}\boldsymbol{\omega_i}\times\mathbf{l_i} \tag{5a}$$

and

$$\dot{\boldsymbol{\rho}}_{mi} = \dot{\boldsymbol{\rho}}_i^* + \frac{m_i}{m_i + m_{mi}}\boldsymbol{\omega_i}\times\mathbf{l_i} \tag{5b}$$

Using (2), (4a), (4b), (5a) and (5b), the angular momentum, given by (1), can be written as follows:

$$\mathbf{h_{CM}} = \sum_{k=0}^{N}\left(\mathbf{I_k^*}\cdot\boldsymbol{\omega_k} + m_k^*\boldsymbol{\rho_k^*}\times\dot{\boldsymbol{\rho}}_k^*\right) + \sum_{k=0}^{N-1}\left(n_{k+1}\dot{\theta}_{mk+1}\mathbf{I_{mk+1}}\cdot\mathbf{z_{mk+1}}\right) \tag{6}$$

where

$$\mathbf{I_k^*} = \mathbf{I_k} + \mathbf{I_{mk+1}} + \frac{m_k m_{mk}}{m_k + m_{mk}}(\mathbf{l_k^\times})^T\cdot\mathbf{l_k^\times} \tag{7a}$$

where the symbol $(\cdot)^\times$ denotes the construction of a skew-symmetric matrix from the components of $(\cdot)$, and

$$m_k^* = m_k + m_{mk} \tag{7b}$$

The first sum of (6) can be written as:

$$\sum_{k=0}^{N}\left(\mathbf{I_k^*}\cdot\boldsymbol{\omega_k} + m_k^*\boldsymbol{\rho_k^*}\times\dot{\boldsymbol{\rho}}_k^*\right) = \mathbf{R_0}(\varepsilon, n)\left({}^{\mathbf{0}}\mathbf{D}^{*\mathbf{0}}\boldsymbol{\omega_0} + {}^{\mathbf{0}}\mathbf{D_q^*}\dot{\mathbf{q}}\right) \tag{8a}$$

where ${}^{\mathbf{0}}\boldsymbol{\omega_0}$ is the spacecraft angular velocity expressed in the spacecraft frame and $\mathbf{R_0}(\varepsilon, n)$ is the rotation matrix between the spacecraft 0th and the inertial frame expressed as a function of the spacecraft unit quaternion ε, n. The inertia-type matrices ${}^{\mathbf{0}}\mathbf{D}^*$ and ${}^{\mathbf{0}}\mathbf{D_q^*}$ are identical in form to the matrices correspond to space manipulators which do not include the motor inertial properties and are given in (Papadopoulos & Dubowsky, 1993). In order to take into account the influence of the motor inertial properties, one has just to replace the variables m_k, $\mathbf{I_k}$, $\mathbf{l_k}$ and $\mathbf{r_k}$ with m_k^*, $\mathbf{I_k^*}$, $\mathbf{l_k^*}$ and $\mathbf{r_k^*}$ given by (3a), (3b), (7a) and (7b). The column vector $\mathbf{q}$ is the link angular position given by

$$\mathbf{q} = \begin{bmatrix} q_1 & q_2 & \cdots & q_N \end{bmatrix}^T \tag{8b}$$

The second sum of (6) is exclusively due to the motor dynamics and is equal to:

$$\sum_{k=0}^{N-1}(n_{k+1}\dot{\theta}_{m_{k+1}}\mathbf{I}_{\mathbf{m_{k+1}}}\cdot\mathbf{z}_{\mathbf{m_{k+1}}}) = \mathbf{R_0}(\varepsilon, n)\,{}^{\mathbf{0}}\mathbf{D}_{\boldsymbol{\theta}_\mathbf{m}}\cdot\dot{\boldsymbol{\theta}}_\mathbf{m} \tag{9a}$$

where the inertia-type matrix ${}^{\mathbf{0}}\mathbf{D}_{\boldsymbol{\theta}_\mathbf{m}}$ is given in Appendix A and the column vector $\boldsymbol{\theta}_\mathbf{m}$ is the gear reduction angular position

$$\boldsymbol{\theta}_\mathbf{m} = \begin{bmatrix}\theta_{m1} & \theta_{m2} & \cdots & \theta_{mN}\end{bmatrix}^T \tag{9b}$$

Finally, the system angular momentum takes the form

$$\mathbf{h_{CM}} = \mathbf{R_0}(\varepsilon, n)({}^{\mathbf{0}}\mathbf{D}^{*}\cdot{}^{\mathbf{0}}\boldsymbol{\omega}_\mathbf{0} + {}^{\mathbf{0}}\mathbf{D}_{\boldsymbol{\Theta}}\cdot\dot{\boldsymbol{\Theta}}) \tag{10}$$

where

$$\boldsymbol{\Theta} = \begin{bmatrix}\mathbf{q}\\ \boldsymbol{\theta}_\mathbf{m}\end{bmatrix} \tag{11a}$$

and

$${}^{\mathbf{0}}\mathbf{D}_{\boldsymbol{\Theta}} = \begin{bmatrix}{}^{\mathbf{0}}\mathbf{D}^{*}_{\mathbf{q}} & {}^{\mathbf{0}}\mathbf{D}_{\boldsymbol{\theta}_\mathbf{m}}\end{bmatrix} \tag{11b}$$

2.2. Motor effect on the system kinetic energy

To obtain the equations of motion of the system, first the system kinetic and potential energy have to be derived.In this section, we study the influence of joint motor inertia properties (mass and moment of inertia) in the total system kinetic energy.

The space manipulator kinetic energy, including motor inertial properties, is given by

$$T = \frac{1}{2}m_0\dot{\boldsymbol{\rho}}_\mathbf{0}\cdot\dot{\boldsymbol{\rho}}_\mathbf{0} + \frac{1}{2}\boldsymbol{\omega}_\mathbf{0}\cdot\mathbf{I}_\mathbf{0}\cdot\boldsymbol{\omega}_\mathbf{0} + \frac{1}{2}\sum_{k=1}^{N}\boldsymbol{\omega}_\mathbf{k}\cdot\mathbf{I}_\mathbf{k}\cdot\boldsymbol{\omega}_\mathbf{k}$$
$$+ \frac{1}{2}\sum_{k=1}^{N}(m_k\dot{\boldsymbol{\rho}}_\mathbf{k}\cdot\dot{\boldsymbol{\rho}}_\mathbf{k} + m_{mk}\dot{\boldsymbol{\rho}}_{\mathbf{mk}}\cdot\dot{\boldsymbol{\rho}}_{\mathbf{mk}}) + \frac{1}{2}\sum_{k=1}^{N}\boldsymbol{\omega}_{\mathbf{mk}}\cdot\mathbf{I}_{\mathbf{mk}}\cdot\boldsymbol{\omega}_{\mathbf{mk}} \tag{12a}$$

Using (2), (4a), (4b), (5a) and (5b), the kinetic energy is simplified as follows:

$$T = \frac{1}{2}\sum_{k=0}^{N}(m^{*}_{\mathbf{k}}\dot{\boldsymbol{\rho}}^{*T}_{\mathbf{k}}\cdot\dot{\boldsymbol{\rho}}^{*}_{\mathbf{k}}) + \frac{1}{2}\sum_{k=0}^{N}(\boldsymbol{\omega}^{T}_{\mathbf{k}}\cdot\mathbf{I}^{*}_{\mathbf{k}}\cdot\boldsymbol{\omega}_\mathbf{k})$$
$$+ \sum_{k=0}^{N-1}(n_{k+1}\dot{\theta}_{m_{k+1}}\boldsymbol{\omega}^{T}_{\mathbf{k}}\cdot\mathbf{I}_{\mathbf{m_{k+1}}}\cdot\mathbf{z}_{\mathbf{m_{k+1}}})$$
$$+ \frac{1}{2}\sum_{k=0}^{N-1}((n_{k+1}\dot{\theta}_{m_{k+1}})^2\mathbf{z}^{T}_{\mathbf{m_{k+1}}}\cdot\mathbf{I}_{\mathbf{m_{k+1}}}\cdot\mathbf{z}_{\mathbf{m_{k+1}}}) \tag{12b}$$

The first two sums of (12b) can be written as follows:

$$\frac{1}{2}\sum_{k=0}^{N}(m^{*}_{\mathbf{k}}\dot{\boldsymbol{\rho}}^{*T}_{\mathbf{k}}\cdot\dot{\boldsymbol{\rho}}^{*}_{\mathbf{k}}) + \frac{1}{2}\sum_{k=0}^{N}(\boldsymbol{\omega}^{T}_{\mathbf{k}}\cdot\mathbf{I}^{*}_{\mathbf{k}}\cdot\boldsymbol{\omega}_\mathbf{k}) =$$
$$\frac{1}{2}{}^{\mathbf{0}}\boldsymbol{\omega}^{T}_{\mathbf{0}}\cdot{}^{\mathbf{0}}\mathbf{D}^{*}\cdot{}^{\mathbf{0}}\boldsymbol{\omega}_\mathbf{0} + {}^{\mathbf{0}}\boldsymbol{\omega}^{T}_{\mathbf{0}}\cdot{}^{\mathbf{0}}\mathbf{D}^{*}_{\mathbf{q}}\cdot\dot{\mathbf{q}} + \frac{1}{2}\dot{\mathbf{q}}^{T}\cdot{}^{\mathbf{0}}\mathbf{D}^{*}_{\mathbf{qq}}\cdot\dot{\mathbf{q}} \tag{13a}$$

where the inertia-type matrix ${}^{\mathbf{0}}\mathbf{D}^{*}_{\mathbf{qq}}$ corresponds to the matrix ${}^{\mathbf{0}}\mathbf{D}_{\mathbf{qq}}$ (Papadopoulos & Dubowsky, 1993) and is obtained by replacing the variables m_k, $\mathbf{I_k}$, $\mathbf{l_k}$ and $\mathbf{r_k}$ with m^{*}_{k}, $\mathbf{I}^{*}_{\mathbf{k}}$, $\mathbf{l}^{*}_{\mathbf{k}}$ and $\mathbf{r}^{*}_{\mathbf{k}}$ given by (3a), (3b), (7a) and (7b).

The third and fourth sum of (12b) can be written, respectively, as follows:

$$\sum_{k=0}^{N-1}(n_{k+1}\dot{\theta}_{m_{k+1}}\boldsymbol{\omega}^{T}_{\mathbf{k}}\cdot\mathbf{I}_{\mathbf{m_{k+1}}}\cdot\mathbf{z}_{\mathbf{m_{k+1}}}) = {}^{\mathbf{0}}\boldsymbol{\omega}^{T}_{\mathbf{0}}\cdot{}^{\mathbf{0}}\mathbf{D}_{\boldsymbol{\theta}_\mathbf{m}}\cdot\dot{\boldsymbol{\theta}}_\mathbf{m} + \dot{\mathbf{q}}^{T}\cdot{}^{\mathbf{0}}\mathbf{D}_{\mathbf{q}\boldsymbol{\theta}_\mathbf{m}}\cdot\dot{\boldsymbol{\theta}}_\mathbf{m} \tag{13b}$$

and

$$\frac{1}{2}\sum_{k=0}^{N-1}((n_{k+1}\dot{\theta}_{m_{k+1}})^2\mathbf{z}^{T}_{\mathbf{m_{k+1}}}\cdot\mathbf{I}_{\mathbf{m_{k+1}}}\cdot\mathbf{z}_{\mathbf{m_{k+1}}}) = \frac{1}{2}\dot{\boldsymbol{\theta}}^{T}_{\mathbf{m}}\cdot\mathbf{D}_{\boldsymbol{\theta}_\mathbf{m}\boldsymbol{\theta}_\mathbf{m}}\cdot\dot{\boldsymbol{\theta}}_\mathbf{m} \tag{13c}$$

where the inertia-type matrices ${}^{\mathbf{0}}\mathbf{D}_{\mathbf{q}\boldsymbol{\theta}_\mathbf{m}}$ and $\mathbf{D}_{\boldsymbol{\theta}_\mathbf{m}\boldsymbol{\theta}_\mathbf{m}}$ are given in Appendix A.

Thus, the kinetic energy of the system takes the form

$$T = \frac{1}{2}{}^{\mathbf{0}}\boldsymbol{\omega}^{\mathbf{T}}_{\mathbf{0}}\cdot{}^{\mathbf{0}}\mathbf{D}^{*}\cdot{}^{\mathbf{0}}\boldsymbol{\omega}_\mathbf{0} + {}^{\mathbf{0}}\boldsymbol{\omega}^{\mathbf{T}}_{\mathbf{0}}\cdot{}^{\mathbf{0}}\mathbf{D}_{\boldsymbol{\Theta}}\cdot\dot{\boldsymbol{\Theta}} + \frac{1}{2}\dot{\boldsymbol{\Theta}}^{\mathbf{T}}\cdot\mathbf{D}_{\boldsymbol{\Theta}\boldsymbol{\Theta}}\cdot\dot{\boldsymbol{\Theta}} \tag{14}$$

where

$$\mathbf{D}_{\boldsymbol{\Theta}\boldsymbol{\Theta}} = \begin{bmatrix}{}^{\mathbf{0}}\mathbf{D}^{*}_{\mathbf{qq}} & {}^{\mathbf{0}}\mathbf{D}_{\mathbf{q}\boldsymbol{\theta}_\mathbf{m}}\\ {}^{\mathbf{0}}\mathbf{D}^{T}_{\mathbf{q}\boldsymbol{\theta}_\mathbf{m}} & \mathbf{D}_{\boldsymbol{\theta}_\mathbf{m}\boldsymbol{\theta}_\mathbf{m}}\end{bmatrix} \tag{15}$$

2.3. Equations of motion

The equations of motion of the system are derived using the Lagrangian approach. The system kinetic energy, including the motor inertial properties, has been determined above. Next, the system potential energy and the dissipation energy are derived.

The potential energy due to gravity is zero. However, the potential energy due to joint flexibility and the dissipation energy are

$$V_{el}(\boldsymbol{\Theta}) = \frac{1}{2}(\boldsymbol{\theta}_\mathbf{m} - \mathbf{q})^{T}\mathbf{K}(\boldsymbol{\theta}_\mathbf{m} - \mathbf{q}) \tag{16a}$$

and

$$D_{dis}(\dot{\boldsymbol{\Theta}}) = \frac{1}{2}(\dot{\boldsymbol{\theta}}_\mathbf{m} - \dot{\mathbf{q}})^{T}\mathbf{B}(\dot{\boldsymbol{\theta}}_\mathbf{m} - \dot{\mathbf{q}}) \tag{16b}$$

where

$$\mathbf{K} = diag\,(k_1, k_2, \ldots, k_N) \tag{17a}$$

and

$$\mathbf{B} = diag\,(b_1, b_2, \ldots, b_N) \tag{17b}$$

The system Lagrangian L defined by

$$L({}^{\mathbf{0}}\boldsymbol{\omega}_\mathbf{0}, \boldsymbol{\Theta}, \dot{\boldsymbol{\Theta}}) = T({}^{\mathbf{0}}\boldsymbol{\omega}_\mathbf{0}, \boldsymbol{\Theta}, \dot{\boldsymbol{\Theta}}) - V_{el}(\boldsymbol{\Theta}) \tag{18a}$$

is written as

$$L(\theta_0, \mathbf{q}, \dot{\mathbf{q}}) = \frac{1}{2}{}^{\mathbf{0}}\boldsymbol{\omega}^{\mathbf{T0}}_{\mathbf{0}}\mathbf{D}^{*\mathbf{0}}\boldsymbol{\omega}_\mathbf{0} + {}^{\mathbf{0}}\boldsymbol{\omega}^{\mathbf{T0}}_{\mathbf{0}}\mathbf{D}_{\boldsymbol{\Theta}}\dot{\boldsymbol{\Theta}} + \frac{1}{2}\dot{\boldsymbol{\Theta}}^{\mathbf{T}}\mathbf{D}_{\boldsymbol{\Theta}\boldsymbol{\Theta}}\dot{\boldsymbol{\Theta}}$$
$$- \frac{1}{2}(\boldsymbol{\theta}_\mathbf{m} - \mathbf{q})^{T}\mathbf{K}(\boldsymbol{\theta}_\mathbf{m} - \mathbf{q}) \tag{18b}$$

Using $[{}^{\mathbf{0}}\boldsymbol{\omega}^{T}_{\mathbf{0}}, \dot{\boldsymbol{\Theta}}^{T}]^{T}$ as the vector of generalized speeds, and employing a quasi-coordinate formulation yields (Nanos & Papadopoulos, 2011):

$$\frac{d}{dt}\left(\frac{\partial T({}^{\mathbf{0}}\boldsymbol{\omega}_\mathbf{0}, \boldsymbol{\Theta}, \dot{\boldsymbol{\Theta}})}{\partial\,{}^{\mathbf{0}}\boldsymbol{\omega}_\mathbf{0}}\right) + {}^{\mathbf{0}}\boldsymbol{\omega}^{\times}_{\mathbf{0}}\frac{\partial T({}^{\mathbf{0}}\boldsymbol{\omega}_\mathbf{0}, \boldsymbol{\Theta}, \dot{\boldsymbol{\Theta}})}{\partial\,{}^{\mathbf{0}}\boldsymbol{\omega}_\mathbf{0}} = \mathbf{R}^{\mathbf{T}}_{\mathbf{0}}\,\mathbf{g_{CM}} \tag{19a}$$

$$\frac{d}{dt}\left(\frac{\partial T({}^{\mathbf{0}}\boldsymbol{\omega}_\mathbf{0}, \boldsymbol{\Theta}, \dot{\boldsymbol{\Theta}})}{\partial\dot{\boldsymbol{\Theta}}}\right) - \frac{\partial T({}^{\mathbf{0}}\boldsymbol{\omega}_\mathbf{0}, \boldsymbol{\Theta}, \dot{\boldsymbol{\Theta}})}{\partial\boldsymbol{\Theta}} + \frac{\partial V_{el}(\boldsymbol{\Theta})}{\partial\boldsymbol{\Theta}} +$$
$$\frac{\partial D_{dis}(\dot{\boldsymbol{\Theta}})}{\partial\dot{\boldsymbol{\Theta}}} = \mathbf{Q} \tag{19b}$$

where $\mathbf{g_{CM}}$ is the vector of the moments of external forces acting on the spacecraft, with respect to the system CM, expressed in the inertial frame and $\mathbf{Q}$ is the vector of generalized forces

$$\mathbf{Q} = \begin{bmatrix}\mathbf{0_{N\times 1}}\\ \mathbf{n}\cdot\boldsymbol{\tau}\end{bmatrix} \tag{19c}$$

where $\mathbf{n}$ is the $N\times N$ diagonal matrix of the joint reduction ratios

$$\mathbf{n} = diag\,(n_1, n_2, \ldots, n_N) \tag{20a}$$

and $\boldsymbol{\tau}$ is the column vector of the motor torques, see Fig. 2:

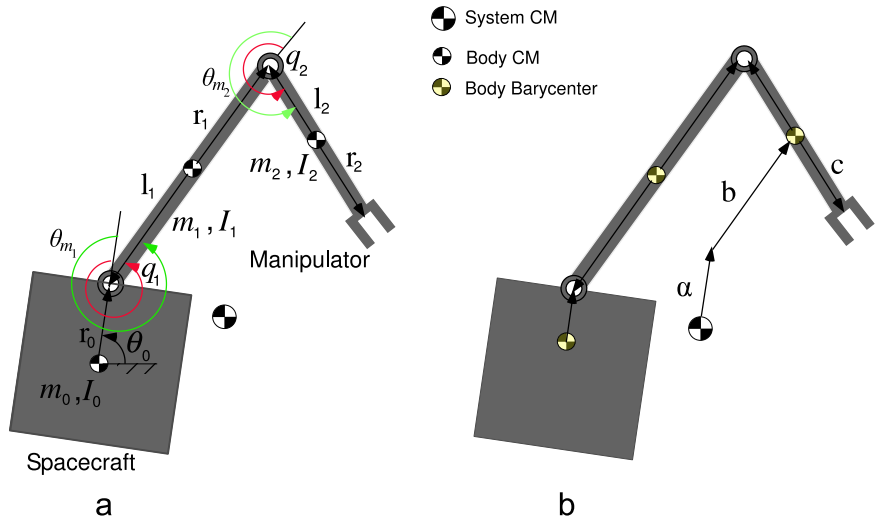

Fig. 4. A planar 7-dof space system.

$$\boldsymbol{\tau} = [\tau_1 \quad \tau_2 \quad \cdots \quad \tau_N]^T \tag{20b}$$

2.3.1. Free-flying mode

In this paper we consider that in the free-flying mode the spacecraft is controlled only by reaction wheels (RW) in order to avoid the thruster fuel consumption. Thus the vector $\mathbf{g_{CM}}$ in (19a) contains only the torques resulting by reaction wheels action.

Combination of (14), (16a), (16b), (19a), (19b) and (19c) yields the following:

$$\mathbf{^0D^{*0}\dot{\omega}_0} + \mathbf{^0D_\Theta\ddot{\Theta}} + \mathbf{C_1^*} = \mathbf{R_0^T g_{CM}} \tag{21a}$$

$$\mathbf{^0D_\Theta^{T0}\dot{\omega}_0} + \mathbf{^0D_{\Theta\Theta}\ddot{\Theta}} + \mathbf{C_2^*} + \begin{bmatrix}\mathbf{-K}\\ \mathbf{K}\end{bmatrix}(\boldsymbol{\theta_m} - \mathbf{q}) + \begin{bmatrix}\mathbf{-B}\\ \mathbf{B}\end{bmatrix}(\dot{\boldsymbol{\theta}}_\mathbf{m} - \dot{\mathbf{q}}) = \mathbf{Q} \tag{21b}$$

where $\mathbf{C_1^*}$ and $\mathbf{C_2^*}$ are the column vectors containing centrifugal and Coriolis forces and are given by

$$\mathbf{C_1^*} = \mathbf{^0\omega_0^\times}(\mathbf{R_0^T}(\varepsilon, n)\mathbf{h_{CM}}) + (\frac{\partial(\mathbf{^0D^{*0}\omega_0})}{\partial\boldsymbol{\Theta}} + \frac{\partial(\mathbf{^0D_\Theta\dot{\Theta}})}{\partial\boldsymbol{\Theta}})\dot{\boldsymbol{\Theta}} \tag{22a}$$

and

$$\mathbf{C_2^*} = [\frac{\partial(\mathbf{^0D_\Theta^{T0}\omega_0})}{\partial\boldsymbol{\Theta}} + \frac{\partial(\mathbf{^0D_{\Theta\Theta}\dot{\Theta}})}{\partial\boldsymbol{\Theta}} - \frac{\partial(\mathbf{^0\omega_0^{T0}D_\Theta})}{\partial\boldsymbol{\Theta}}]\dot{\boldsymbol{\Theta}} - \frac{1}{2}\frac{\partial(\dot{\boldsymbol{\Theta}}^{\mathbf{T0}}\mathbf{D_{\Theta\Theta}})}{\partial\boldsymbol{\Theta}}\dot{\boldsymbol{\Theta}} - \frac{1}{2}\frac{\partial(\mathbf{^0\omega_0^{T0}D^*})}{\partial\boldsymbol{\Theta}}\mathbf{^0\omega_0} \tag{22b}$$

2.3.2. Free-floating mode

In the case of free-floating manipulators, the moments of external forces acting on the spacecraft are equal to zero, i.e. $\mathbf{g_{CM}} = \mathbf{0}$, and the angular momentum $\mathbf{h_{CM}}$ defined in (10) is constant. We assume that the angular momentum is zero.

Solving (21a) for $\mathbf{^0\dot{\omega}_0}$ and substituting in (21b) yields,

$$\mathbf{H^*(\Theta)\ddot{\Theta}} + \begin{bmatrix}\mathbf{C_1(q,\dot{\Theta})}\\ \mathbf{C_2(q,\dot{\Theta})}\end{bmatrix} + \begin{bmatrix}\mathbf{-K}\\ \mathbf{K}\end{bmatrix}(\boldsymbol{\theta_m} - \mathbf{q}) + \begin{bmatrix}\mathbf{-B}\\ \mathbf{B}\end{bmatrix}(\dot{\boldsymbol{\theta}}_\mathbf{m} - \dot{\mathbf{q}}) = \mathbf{Q} \tag{23}$$

where the inertia matrix $\mathbf{H^*(\Theta)}$ is given by

$$\mathbf{H^*(\Theta)} = \mathbf{^0D_{\Theta\Theta}} - \mathbf{^0D_\Theta^T(^0D_*)^{-1}{}^0D_\Theta} = \begin{bmatrix}\mathbf{H_{qq}^*} & \mathbf{H_{q\theta m}}\\ \mathbf{H_{q\theta m}^T} & \mathbf{H_{\theta m\theta m}}\end{bmatrix} \tag{24a}$$

and the column vector of centrifugal and Coriolis forces is

$$\mathbf{C(^0\omega_0, \Theta, \dot{\Theta})} = \mathbf{C_2^*} - \mathbf{^0D_\Theta^T(^0D_*)^{-1}C_1^*} \tag{24b}$$

Then, substituting the vector $\mathbf{^0\omega_0}$ from (10) in (24b) results in

$$\mathbf{C} = \begin{bmatrix}\mathbf{C_1}\\ \mathbf{C_2}\end{bmatrix} = [\frac{1}{2}\frac{\partial(\dot{\boldsymbol{\Theta}}^{T}\mathbf{^0D_\Theta^T(^0D_*)^{-T}{}^0D_\Theta})}{\partial\boldsymbol{\Theta}} + \frac{\partial(\mathbf{^0D_{\Theta\Theta}\dot{\Theta}})}{\partial\boldsymbol{\Theta}}]\dot{\boldsymbol{\Theta}} - [\frac{1}{2}\frac{\partial(\dot{\boldsymbol{\Theta}}^{T}\mathbf{^0D_{\Theta\Theta}})}{\partial\boldsymbol{\Theta}} + \frac{\partial(\mathbf{^0D_\Theta^T\cdot(^0D^*)^{-1}{}^0D_\Theta\dot{\Theta}})}{\partial\boldsymbol{\Theta}}]\dot{\boldsymbol{\Theta}} \tag{24c}$$

To use these equations of motion, in controller design, they are written in the following form of link and motor equations:

$$\mathbf{H_{qq}(q)\ddot{q}} + \mathbf{H_{q\theta m}(q)\ddot{\theta}_m} + \mathbf{h_1(\Theta, \dot{\Theta})} = \mathbf{0} \tag{25a}$$

$$\mathbf{H_{q\theta m}^T(q)\ddot{q}} + \mathbf{H_{\theta m\theta m}(q)\ddot{\theta}_m} + \mathbf{h_2(\Theta, \dot{\Theta})} = \mathbf{n\cdot\tau} \tag{25b}$$

where

$$\mathbf{h_1(\Theta, \dot{\Theta})} = \mathbf{C_1(q, \dot{\Theta})} - \mathbf{K}(\boldsymbol{\theta_m} - \mathbf{q}) - \mathbf{B}(\dot{\boldsymbol{\theta}}_\mathbf{m} - \dot{\mathbf{q}}) \tag{26a}$$

and

$$\mathbf{h_2(\Theta, \dot{\Theta})} = \mathbf{C_2(q, \dot{\Theta})} + \mathbf{K}(\boldsymbol{\theta_m} - \mathbf{q}) + \mathbf{B}(\dot{\boldsymbol{\theta}}_\mathbf{m} - \dot{\mathbf{q}}) \tag{26b}$$

Thus, under the assumptions of free-floating systems, the equations of motion of a flexible joint space manipulator system with uncontrolled spacecraft can be reduced from $2N+6$ to just $2N$, that is as many as the flexible joint manipulator dof.

2.4. Planar manipulators

In the case of planar systems, such as the 7-dof (i.e. 2-dof for each flexible joint and 3-dof for the spacecraft) system shown in Fig. 4, the equations of motion can be simplified. The corresponding equations used for the free-flying and the free-floating modes are given next.

2.4.1. Free-flying mode

As mentioned above, in this paper we consider that in the free-flying mode the spacecraft is controlled only by reaction wheels. Eqs. (21a) and (21b) can be written in a matrix form:

$$\begin{bmatrix} {}^0D^* & \mathbf{^0D_\Theta} \\ \mathbf{^0D_\Theta^T} & \mathbf{^0D_{\Theta\Theta}} \end{bmatrix} \begin{bmatrix} \ddot{\theta}_0 \\ \ddot{\mathbf{\Theta}} \end{bmatrix} + \begin{bmatrix} c_1^* \\ \mathbf{C_2^*} \end{bmatrix} + \begin{bmatrix} \mathbf{0_{1\times N}} \\ -\mathbf{K} \\ \mathbf{K} \end{bmatrix} (\boldsymbol{\theta_m} - \mathbf{q}) + \begin{bmatrix} \mathbf{0_{1\times N}} \\ -\mathbf{B} \\ \mathbf{B} \end{bmatrix} (\dot{\boldsymbol{\theta}}_\mathbf{m} - \dot{\mathbf{q}}) = \begin{bmatrix} \tau_{rw} \\ \mathbf{Q} \end{bmatrix} \tag{27}$$

where τ_{rw} is the torque acting on the spacecraft by the RW, θ_0 denotes the spacecraft attitude and the inertia type matrices ${}^0D^*$, $\mathbf{^0D_\Theta}$ and $\mathbf{^0D_{\Theta\Theta}}$ for the 7-dof planar manipulator shown in Fig. 4, are given in Appendix B.

Note that in planar space manipulators, the vectors $\mathbf{^0\omega_0}$ and $\mathbf{^0h_{CM}}$ (as well as the vector $\mathbf{h_{CM}}$) are parallel (the direction of both vector is normal to the motion plane). Therefore, the cross product of these vectors appears in (22a) is equal to zero and (22a) takes the form

$$\mathbf{C_1^*}(\dot{\theta}_0, \mathbf{\Theta}, \dot{\mathbf{\Theta}}) = \left(\frac{\partial(\mathbf{^0D^*}\dot{\theta}_0)}{\partial \mathbf{\Theta}} + \frac{\partial(\mathbf{^0D_\Theta}\dot{\mathbf{\Theta}})}{\partial \mathbf{\Theta}}\right)\dot{\mathbf{\Theta}} \tag{28}$$

For the 7-dof manipulator in Fig. 4, it can be shown that (28) and (22b) can be written as:

$$\begin{aligned} \mathbf{C_1^*}(\dot{\theta}_0, \mathbf{q}, \dot{\mathbf{q}}) = &- (\hat{d}_{01}^* + \hat{d}_{02}^*)(2\dot{\theta}_0\dot{q}_1 + \dot{q}_1^2) \\ &- (\hat{d}_{12}^* + \hat{d}_{02}^*)(2\dot{\theta}_0\dot{q}_2 + 2\dot{q}_1\dot{q}_2 + \dot{q}_2^2) \end{aligned} \tag{29a}$$

and

$$\mathbf{C_2^*}(\dot{\theta}_0, \mathbf{q}, \dot{\mathbf{q}}) = \begin{bmatrix} -\hat{d}_{12}^*(2\dot{q}_1\dot{q}_2 + 2\dot{\theta}_0\dot{q}_2 + \dot{q}_2^2) + (\hat{d}_{01}^* + \hat{d}_{02}^*)\dot{\theta}_0^2 \\ \hat{d}_{12}^*(2\dot{\theta}_0\dot{q}_1 + \dot{q}_1^2) + (\hat{d}_{12}^* + \hat{d}_{02}^*)\dot{\theta}_0^2 \\ 0 \\ 0 \end{bmatrix} \tag{29b}$$

where the terms $\hat{d}_{ij}^*$ are functions of $\mathbf{q}$ and defined in Appendix B.

2.4.2. Free-floating mode

In the free-floating mode, the equations of motion for both planar and spatial systems are given by (23), repeated here,

$$\mathbf{H^*}(\mathbf{\Theta})\ddot{\mathbf{\Theta}} + \mathbf{C}(\mathbf{q}, \dot{\mathbf{\Theta}}) + \begin{bmatrix} -\mathbf{K} \\ \mathbf{K} \end{bmatrix}(\boldsymbol{\theta_m} - \mathbf{q}) + \begin{bmatrix} -\mathbf{B} \\ \mathbf{B} \end{bmatrix}(\dot{\boldsymbol{\theta}}_\mathbf{m} - \dot{\mathbf{q}}) = \mathbf{Q}$$

where $\mathbf{H^*}(\mathbf{\Theta})$ is the inertia matrix and $\mathbf{C}(\mathbf{q}, \dot{\mathbf{\Theta}})$ is the column vector of the centrifugal and Coriolis forces given by (24a) and (24c), respectively. The inertia type matrices $\mathbf{H_{qq}^*}$, $\mathbf{H_{q\theta_m}}$ and $\mathbf{H_{\theta_m\theta_m}}$ used in (24a), for the planar 7-dof manipulator shown in Fig. 4, are given in Appendix C.

Note that the column vector of the centrifugal and Coriolis forces can be found by (24b), as well. However, in planar free-floating manipulators with no external forces or torques, the vector of angular momentum is constant, and therefore the column vector given by (22a) is zero:

$$\mathbf{C_1^*}(\dot{\theta}_0, \mathbf{\Theta}, \dot{\mathbf{\Theta}}) = \frac{\partial(\mathbf{^0D^*}\dot{\theta}_0 + \mathbf{^0D_\Theta}\dot{\mathbf{\Theta}})}{\partial \mathbf{\Theta}}\dot{\mathbf{\Theta}} = \frac{\partial(\mathbf{^0h_{CM}})}{\partial \mathbf{\Theta}}\dot{\mathbf{\Theta}} = \mathbf{0} \tag{30a}$$

Therefore, vector $\mathbf{C}$ reduces to,

$$\mathbf{C}(\dot{\theta}_0, \mathbf{q}, \dot{\mathbf{q}}) = \mathbf{C_2^*}(\dot{\theta}_0, \mathbf{q}, \dot{\mathbf{q}}) \tag{30b}$$

where the column vector $\mathbf{C_2^*}(\dot{\theta}_0, \mathbf{q}, \dot{\mathbf{q}})$, for the planar 7-dof manipulator shown in Fig. 4, is given by (29b) and the spacecraft angular velocity $\dot{\theta}_0$ results from the angular momentum conservation. Assuming zero initial angular momentum, (10) takes the following form:

$$\dot{\theta}_0 = \frac{1}{{}^0D^*}\mathbf{^0D_\Theta}\dot{\mathbf{\Theta}} \tag{30c}$$

where the term ${}^0D^*$, and the matrix $\mathbf{^0D_\Theta}$, for the planar 7-dof manipulator shown in Fig. 4, are given in Appendix B.

2.5. Comparison with fixed-base manipulators

The coupling matrix $\mathbf{H_{q\theta_m}}(\mathbf{q})$, which appears in (25a) and (25b), represents the inertial coupling between motor and link accelerations. According to the assumption (iii), the motor i is mounted on link $i-1$ and rotates link i. Since, in fixed-base manipulators, the velocity (linear and/or angular) of motor i is independent of the motion of the link i and the subsequent ones, the matrix $\mathbf{H_{q\theta_m}}(\mathbf{q})$ always has the following strictly upper-triangular structure (De Luca, 1998):

$$\mathbf{H_{q\theta_m}} = \begin{bmatrix} 0 & h_{12} & h_{13}(q_2) & h_{14}(q_2, q_3) & \cdots & \cdots & h_{1N}(q_2, \ldots, q_{N-1}) \\ 0 & 0 & h_{23} & h_{24}(q_3) & \cdots & \cdots & h_{2N}(q_3, \ldots, q_{N-1}) \\ 0 & 0 & 0 & h_{34} & \cdots & \cdots & h_{3N}(q_4, \ldots, q_{N-1}) \\ \vdots & \vdots & \vdots & \ddots & \ddots & \vdots & \vdots \\ 0 & 0 & 0 & \cdots & 0 & h_{N-2,N-1} & h_{N-2,N}(q_{N-1}) \\ 0 & 0 & 0 & \cdots & 0 & 0 & h_{N-1,N} \\ 0 & 0 & 0 & \cdots & 0 & 0 & 0 \end{bmatrix} \tag{31a}$$

However, in space robotic systems, any motion of a single link creates a reactional motion in the whole system. Thus, in free-floating space manipulators, the coupling matrix $\mathbf{H_{q\theta_m}}(\mathbf{q})$ does not have a strictly upper- triangular structure. For example, the coupling matrix $\mathbf{H_{q\theta_m}}(\mathbf{q})$ for a 7-dof planar free-floating manipulator is:

$$\mathbf{H_{q\theta_m}} = \begin{bmatrix} -\dfrac{({}^0D_1^* + {}^0D_2^*)n_1 I_{m1}}{{}^0D^*} & n_2 I_{m2} - \dfrac{({}^0D_1^* + {}^0D_2^*)n_2 I_{m2}}{{}^0D^*} \\ -\dfrac{{}^0D_2^* n_1 I_{m1}}{{}^0D^*} & -\dfrac{{}^0D_2^* n_2 I_{m2}}{{}^0D^*} \end{bmatrix} \tag{31b}$$

Note that, when the spacecraft mass and moment of inertia approach to infinity,

$$m_0 \to \infty, \quad I_0 \to \infty \tag{32a}$$

Then

$$\begin{aligned} &\frac{D_1}{D} \to 0, \quad \frac{D_2}{D} \to 0, \quad \frac{I_{m1}}{D} \to 0, \quad \frac{I_{m2}}{D} \to 0, \\ &\frac{m_1}{D} \to 0, \quad \frac{m_2}{D} \to 0, \quad \frac{m_{m1}}{D} \to 0, \quad \frac{m_{m2}}{D} \to 0 \end{aligned} \tag{32b}$$

Application of the above limits in the inertia matrices $\mathbf{H_{qq}^*}$, $\mathbf{H_{q\theta_m}}$ and $\mathbf{H_{\theta_m\theta_m}}$ of a 7-dof planar free-floating manipulator, given in Appendix C, results in the following matrices

$$\mathbf{H_{qq}} = \begin{bmatrix} h_{11} & h_{12} \\ h_{12} & h_{22} \end{bmatrix} \tag{33a}$$

$$\mathbf{H_{q\theta_m}} = \begin{bmatrix} 0 & n_2 I_{m2} \\ 0 & 0 \end{bmatrix} \tag{33b}$$

$$\mathbf{H_{\theta_m\theta_m}} = \begin{bmatrix} n_1^2 I_{m1} & 0 \\ 0 & n_2^2 I_{m2} \end{bmatrix} \tag{33c}$$

where the terms h_{ij} in (33a) are given in Appendix D.

The above matrices are identical to those for a 4-dof fixed-base flexible joint planar manipulator (De Luca, 1998).

3. Control issues of flexible joint space manipulators

This section deals with the control issues of flexible-joint space

Table 1
Parameters of the 3 body planar system.

Body	m_i (kg)	l_i (m)	r_i (m)	I_i (kg m^2)
0	4000	5.0	5.0	666.7
1	200	5.0	5.0	33.3
2	1000	2.5	2.5	50.0

Table 2
Parameters of the motors and the drive mechanisms.

Motor	n_i	k_i (Nm/rad)	b_i (Nms/rad)	m_{mi} (kg)	I_{mi} (kg m^2)
1	50	1000	14.1	1.0	0.00002
2	50	1000	14.1	1.0	0.00002

manipulators. Like fixed-base manipulators, the basic control problems of flexible-joint space manipulators are the regulation control, where the manipulator is driven to a desired final configuration, and the trajectory tracking control where time-varying trajectories are commanded to be followed by the manipulator.

In fixed-base applications, for the regulation control problem a PID control law based on motor feedback can be used

$$\boldsymbol{\tau_m} = \mathbf{K_p e_m} + \mathbf{K_d}\dot{\mathbf{e}}_\mathbf{m} + \mathbf{K_I}\int_0^t \mathbf{e_m}\, dt \tag{34a}$$

where

$$\mathbf{e_m} = \boldsymbol{\theta}_{m,\mathbf{d}} - \boldsymbol{\theta_m} \tag{34b}$$

is the position error at the output of the gear reducer, $\boldsymbol{\theta}_{m,\mathbf{d}}$ is the desired angle at the output of the gear reducer, and $\mathbf{K_p}$, $\mathbf{K_d}$ and $\mathbf{K_I}$ are diagonal positive-definite gain matrices.

However in space applications, the use of the above controller is inadequate. It is well-known that, in free-floating mode, dynamic coupling between manipulator and spacecraft exists and therefore manipulator motions induce disturbances to the spacecraft. Thus, the oscillation motion of manipulator causes an undesirable oscillatory motion of the spacecraft, as shown via the next example.

Example 1: The planar 7-dof free-floating manipulator system with parameters in Table 1 is employed. The motor inertial properties as well as the properties of the flexible drive mechanism are presented in Table 2.

The initial configuration of the manipulator is $(q_{1,in}, q_{2,in}) = (0^o, 30^o)$ and the initial spacecraft attitude is $\theta_{0,in} = 0^o$. The desired final configuration of the manipulator is $(q_{1,fin}, q_{2,fin}) = (100^o, 60^o)$. The manipulator is driven to the final desired configuration in time $t_f = 100\,s$ with zero initial and final velocities and accelerations. The final spacecraft attitude is resulted by the angular momentum conservation.

A PID control law is applied, given by (34a). Application of the torque balance on the rotor and link, see Fig. 2, neglecting the joint deflection (i.e. $\theta_m = q$) and considering both viscous and coulomb friction, results, respectively, in:

$$\tau = \tau_m - I_m n\ddot{\theta}_m - b_m n\dot{\theta}_m - \tau_{c,m}\,\mathrm{sgn}\,(n\dot{\theta}_m) \tag{35a}$$

and

$$n\tau = I_L\ddot{\theta}_m + b_L\dot{\theta}_m + \tau_{c,L}\,\mathrm{sgn}\,(\dot{\theta}_m) \tag{35b}$$

where b_m and $\tau_{c,m}$ are the viscous friction and the coulomb friction motor parameters, respectively, while b_L and $\tau_{c,L}$ are the viscous friction and the coulomb friction link parameters.

The motor torque τ_m is given by (34a) which for a single link takes the form

$$\tau_m = k_p e_m + k_d\dot{e}_m + k_I\int_0^t e_m\, dt \tag{35c}$$

The combination of (35a)–(35c) results in the error dynamics which is given by

$$\ddot{e}_m + \frac{n\,k_d + b_e}{I_e}\ddot{e}_m + \frac{n\,k_p}{I_e}\dot{e}_m + \frac{n\,k_i}{I_e}e_m = \ddot{\theta}_m^d + \frac{b_e}{I_e}\ddot{\theta}_m^d \tag{36a}$$

where the values of $\dddot{\theta}_m^d$ and $\ddot{\theta}_m^d$ are zero at the steady state and J_e, b_e are the effective inertia and effective damping, respectively, both seen at the link side of the gear and given by

$$I_e = n^2 I_m + I_L \tag{36b}$$

where I_L represents the moment of inertia of a link with respect to its joint closer to the base and

$$b_e = n^2\, b_m + b_L \tag{36c}$$

The error dynamics, described by (36a), is linear and the desired characteristic equation can be chosen as

$$\begin{aligned} p_d(s) &= (s+a)(s+w)^2 \\ &= s^3 + (a+2w)s^2 + (2aw + w^2)s + aw^2 \end{aligned} \tag{37}$$

where $w > 0$ and $a \geq 5\,w$ are the locations of the desired poles which correspond to a critical damped second order system, i.e. $\zeta = 1$.

The combination of the above equations yield the following PID controller gains:

$$k_p = (2aw + w^2)I_e/n \tag{38a}$$

$$k_d = ((a+2w)I_e - b_e)/n \tag{38b}$$

$$k_i = aw^2 I_e/n \tag{38c}$$

To avoid exciting resonances, the closed-loop natural frequency $\omega_{n,cl}$, i.e. the location of the desired pole w, should satisfy the following condition:

$$\frac{6}{t_s} < \omega_{n,cl} < \frac{1}{5}\omega_{res} \tag{39a}$$

where t_s is the settling time of the desired response and ω_{res} is the resonant frequency given by

$$\omega_{res} = \sqrt{k/\bar{I}} \tag{39b}$$

where $\bar{I}$ is the equivalent reduced inertia defined as

$$\bar{I} = \frac{n^2 I_m I_L}{n^2 I_m + I_L} \tag{39c}$$

Fig. 5 shows the block diagram of the closed-loop system of Example 1, which represents the proposed PID controller applied to the space manipulator with flexible joints and actuator dynamics.

The selected gain matrices of the PID control input are

$$\mathbf{K_P} = \begin{bmatrix} 26.4 & 0 \\ 0 & 5.5 \end{bmatrix},\quad \mathbf{K_D} = \begin{bmatrix} 167.9 & 0 \\ 0 & 34.9 \end{bmatrix},\quad \mathbf{K_I} = \begin{bmatrix} 1.2 & 0 \\ 0 & 0.25 \end{bmatrix} \tag{40}$$

Figs. 6 and 7 show the manipulator oscillating motion and the corresponding vibration of the spacecraft. The low frequency in the response of the manipulator is normal to space systems whose frequencies are usually in the vicinity of 1 Hz. The resulting spacecraft vibration may cause faulty function of several appendages mounted on it such the communication antenna and the

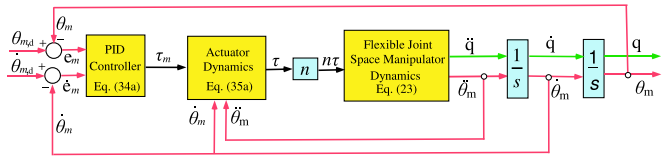

Fig. 5. The block diagram of the closed-loop system of Example 1.

solar panels. Fig. 8 shows the required motor torques.

To reject undesirable spacecraft oscillations, reaction wheels can be used. Then, the spacecraft dynamics can be written as follows:

$$I_0\ddot{\theta}_0 = \tau_{rw} + T \tag{41a}$$

where T is the torque resulting from the manipulator motion, and τ_{rw} is the torque applied by the reaction wheel of the spacecraft, which has the form of a PID controller:

$$\tau_{rw} = k_p(\theta_{0,d} - \theta_0) + k_d(\dot{\theta}_{0,d} - \dot{\theta}_0) + k_i \int_0^t (\theta_{0,d} - \theta_0)dt \tag{41b}$$

where $\theta_{0,d}$ is the desired spacecraft attitude.

Assuming constant torque T, the error dynamics of the spacecraft attitude, resulting from the combination of (41a) and (41b), is

$$\ddot{e}_0 + \frac{k_d}{I_0}\ddot{e}_0 + \frac{k_p}{I_0}\dot{e}_0 + \frac{k_i}{I_0}e_0 = 0 \tag{41c}$$

where $e_0 = \theta_{0,d} - \theta_0$ is the spacecraft attitude error.

Applying the same procedure as above, one can select the control law gains as $k_p = 7.3{\cdot}10^3$, $k_d = 4.7{\cdot}10^3$, $k_i = 3.3{\cdot}10^3$. The desired motion and control is the same as in Example 1. The resulting motions of the spacecraft and the manipulator are shown in Fig. 9. Although the RW controller establishes the desired spacecraft motion, the manipulator oscillations have increased.

It is obvious that a control law, able to achieve non-oscillatory motions for both the spacecraft and its manipulator, is needed. In addition, it is desired often that the end-effector can follow a predefined path. Thus, the proposed control law also should achieve end-effector trajectory tracking.

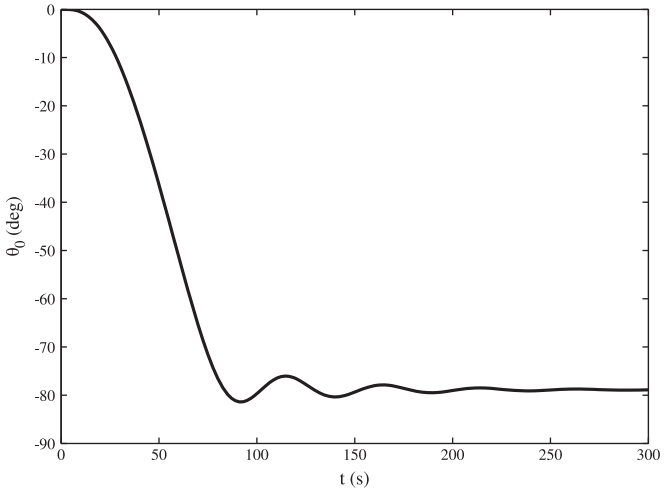

Fig. 7. The oscillatory motion of the spacecraft.

In fixed-base, flexible joint manipulators, the problem of end-effector trajectory tracking has been addressed by using dynamic feedback linearization controllers whose computational effort is unfeasible for space applications. A static feedback linearization controller with much less computation effort (i.e. feasible in space applications) can be applied only if a reduced model is considered, due to the strictly upper- triangular structure of the coupling matrix $\mathbf{H_{q\theta_m}}$, see (31a). However, the reduced model is not a realistic one in most cases since it assumes that the kinetic energy of each rotor is due only to its own rotation.

However, the non-strictly upper-triangular structure of the coupling matrix $\mathbf{H_{q\theta_m}}$ in free-floating space manipulators, see (31b) for 7-dof planar one, gives new opportunities in the design of trajectory following controllers.

Next, we exploit the structure of the derived dynamics, and we propose a static feedback linearization control law, which can be applied for path planning both in the joint and Cartesian spaces,

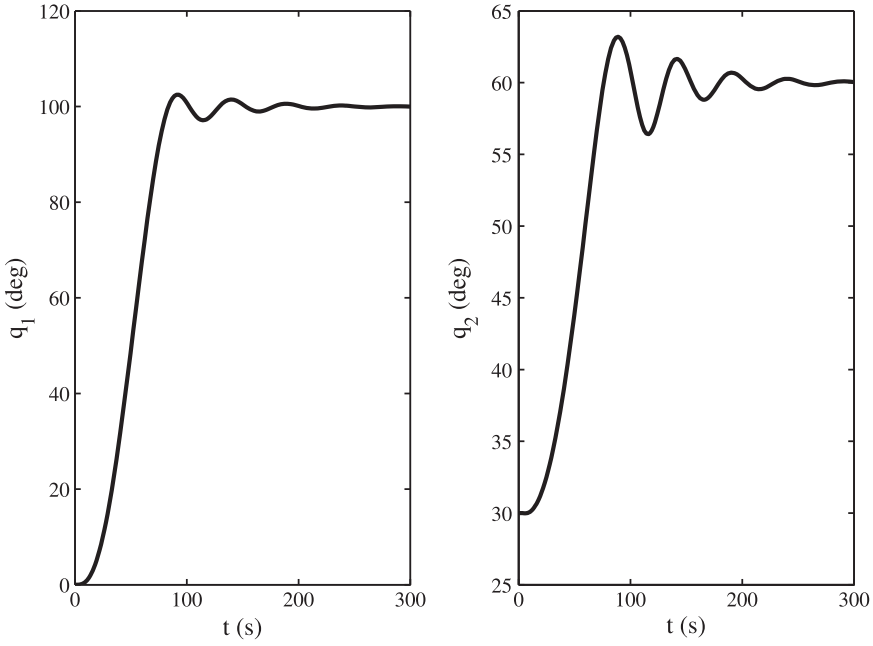

Fig. 6. The oscillatory motion of the manipulator.

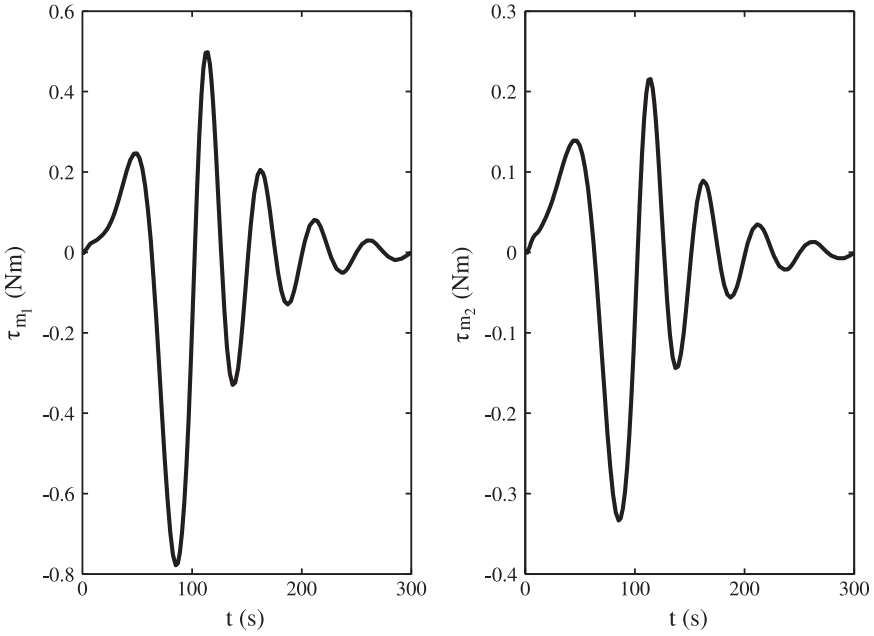

Fig. 8. Motor torques for driving the manipulator to the desired configuration.

also resulting in a non-oscillatory spacecraft motion.

4. Static feedback linearization control law

In this section, we develop a static feedback linearization control law to decouple the link and the motor equations, given by (25a) and (25b), for a spatial free-floating space manipulator. However, since (25a) has not any control input, one cannot control both link configuration $\mathbf{q}$ and the gear reduction angular position $\boldsymbol{\theta}_\mathbf{m}$. Therefore, next only the control of link configuration $\mathbf{q}$ is proposed and the gear reduction angular position $\boldsymbol{\theta}_\mathbf{m}$ remains uncontrolled. The required stability of $\boldsymbol{\theta}_\mathbf{m}$ is examined considering the internal dynamics of the system.

Eq. (25b) can be solved as

$$\ddot{\boldsymbol{\theta}}_\mathbf{m} = \mathbf{H}^{-1}_{\boldsymbol{\theta}_\mathbf{m}\boldsymbol{\theta}_\mathbf{m}}(\mathbf{q})(\mathbf{u} - \mathbf{H}^{T}_{\mathbf{q}\boldsymbol{\theta}_\mathbf{m}}(\mathbf{q})\ddot{\mathbf{q}} - \mathbf{h_2}(\boldsymbol{\Theta}, \dot{\boldsymbol{\Theta}})) \tag{42a}$$

where

$$\mathbf{u} = \mathbf{n}\cdot\boldsymbol{\tau} \tag{42b}$$

and combining with (25a), one finally yields:

$$\ddot{\mathbf{q}} = \mathbf{A}(\mathbf{q})\mathbf{u} + \mathbf{G}(\boldsymbol{\Theta}, \dot{\boldsymbol{\Theta}}) \tag{43}$$

where $\mathbf{A}(\mathbf{q})$, called the decoupling matrix, is given by

$$\mathbf{A}(\mathbf{q}) = -\mathbf{S}^{-1}(\mathbf{q})\mathbf{H}_{\mathbf{q}\boldsymbol{\theta}_\mathbf{m}}(\mathbf{q})\mathbf{H}^{-1}_{\boldsymbol{\theta}_\mathbf{m}\boldsymbol{\theta}_\mathbf{m}}(\mathbf{q}) \tag{44a}$$

and

$$\mathbf{G}(\boldsymbol{\Theta}, \dot{\boldsymbol{\Theta}}) = -\mathbf{A}(\mathbf{q})\mathbf{h_2}(\boldsymbol{\Theta}, \dot{\boldsymbol{\Theta}}) - \mathbf{S}^{-1}(\mathbf{q})\mathbf{h_1}(\boldsymbol{\Theta}, \dot{\boldsymbol{\Theta}}) \tag{44b}$$

and

$$\mathbf{S}(\mathbf{q}) = \mathbf{H}_{\mathbf{qq}}(\mathbf{q}) - \mathbf{H}_{\mathbf{q}\boldsymbol{\theta}_\mathbf{m}}(\mathbf{q})\mathbf{H}^{-1}_{\boldsymbol{\theta}_\mathbf{m}\boldsymbol{\theta}_\mathbf{m}}(\mathbf{q})\mathbf{H}^{T}_{\mathbf{q}\boldsymbol{\theta}_\mathbf{m}}(\mathbf{q}) \tag{44c}$$

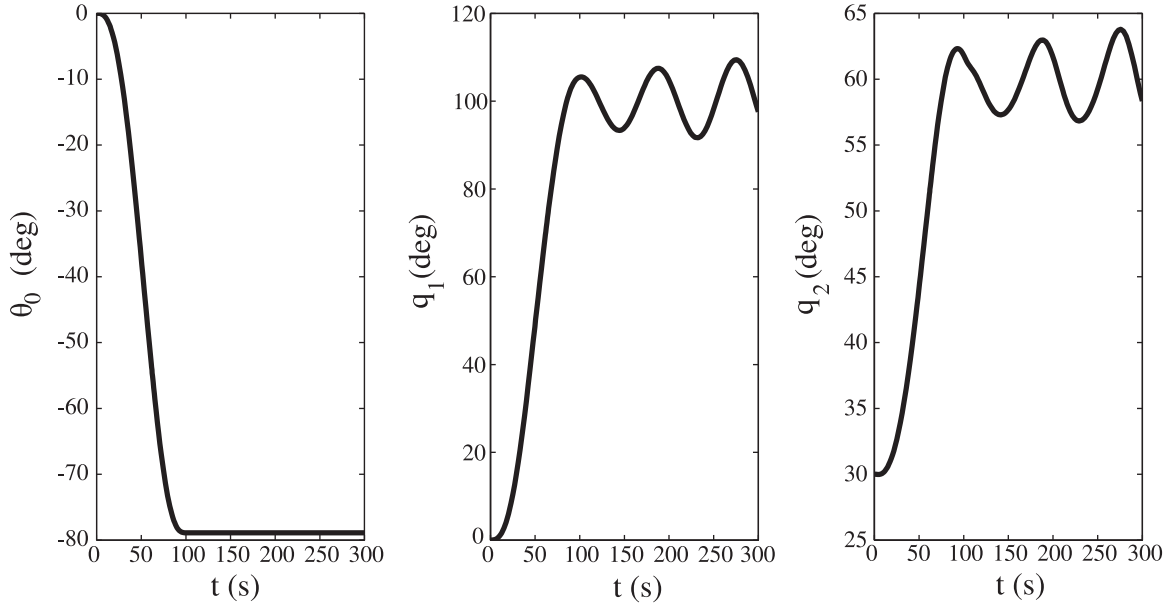

Fig. 9. The oscillating motion of the manipulator.

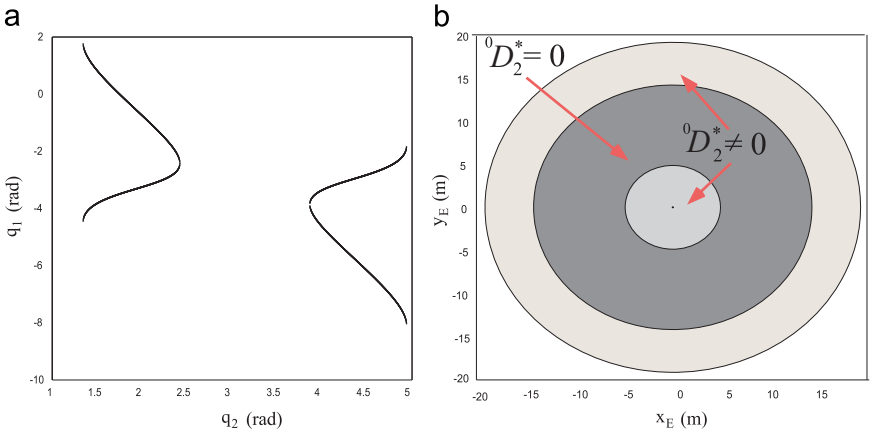

Fig. 10. (a) Manipulator configurations and (b) workspace areas where ${}^0D_2^* = 0$.

Then the following model-based control law

$$\mathbf{u} = \mathbf{A}^{-1}(\mathbf{q})(-\mathbf{G}(\Theta, \dot{\Theta}) + \ddot{\mathbf{q}}_\mathbf{d} + \mathbf{K_P e} + \mathbf{K_d}\dot{\mathbf{e}} + \mathbf{K_I}\int_0^t \mathbf{e}\, dt) \tag{45}$$

decouples the system and the error dynamics is written as

$$\ddot{\mathbf{e}} + \mathbf{K_d}\ddot{\mathbf{e}} + \mathbf{K_P}\dot{\mathbf{e}} + \mathbf{K_I}\mathbf{e} = \mathbf{0} \tag{46a}$$

where $\mathbf{e} = \mathbf{q_d} - \mathbf{q}$ is the manipulator joint error.

Thus, the selection of the diagonal positive definite gain matrices $\mathbf{K_p}$, $\mathbf{K_d}$ and $\mathbf{K_I}$ such that their elements satisfy the condition

$$k_{di}k_{pi} > k_i \tag{46b}$$

shows that the joint error will converge to zero, asymptotically.

Note that the control law, given by (45), is applicable only if the decoupling matrix $\mathbf{A}(\mathbf{q})$, given by (44a), has full rank. In free-floating space manipulators, there are configurations $\mathbf{q}$ for which the matrix $\mathbf{A}(\mathbf{q})$ is invertible. For example, in a 7-dof planar system the determinant of $\mathbf{A}(\mathbf{q})$ is not zero when:

$${}^0D_2^* \neq 0 \Rightarrow a_{20}^* \cos(q_1 + q_2) + a_{21}^* \cos(q_2) + a_{22}^* \neq 0 \tag{47}$$

where a_{20}^*, a_{21}^* and a_{22}^* are constant terms given in Appendix A.

Thus, if the desired path satisfies (47), a static feedback controller will decouple the system. In case where (47) is not satisfied, i.e. ${}^0D_2^* = 0$, the coupling matrix $\mathbf{H_{q\theta_m}}$, see (31b), is not of full rank. According to (44a), this results in the loss of full rank of the decoupling matrix $\mathbf{A}(\mathbf{q})$. Then, as results by (43), there are some joint accelerations which are not affected no matter what joint torques $\mathbf{u}$ are selected.

Fig. 10a presents the manipulator configurations where ${}^0D_2^* = 0$, and Fig. 10b the workspace areas where these configurations may appear.

The proposed controller can achieve tracking of desired time-varying trajectories of the configuration $\mathbf{q}$. However, in space applications, the end-effector position is not only a function of manipulator configuration $\mathbf{q}$ but also depends on the spacecraft attitude (Nanos & Papadopoulos, 2012). In the free-floating mode, the spacecraft attitude is derived by the spacecraft angular velocity resulting from the conversation of angular momentum. For zero initial angular momentum, (10) is written as

$${}^\mathbf{0}\boldsymbol{\omega}_\mathbf{0} = -{}^\mathbf{0}\mathbf{D}^{*-1}({}^\mathbf{0}\mathbf{D}_\mathbf{q}^*\dot{\mathbf{q}} + {}^\mathbf{0}\mathbf{D}_{\boldsymbol{\theta}_\mathbf{m}}\dot{\boldsymbol{\theta}}_\mathbf{m}) \tag{48}$$

So, the spacecraft attitude depends on the uncontrolled gear reduction speed $\dot{\boldsymbol{\theta}}_\mathbf{m}$. However, the effect of the term which consists the uncontrolled gear reduction speed $\dot{\boldsymbol{\theta}}_\mathbf{m}$ in the above equation is too small compared to the other term because the inertia-type matrix ${}^\mathbf{0}\mathbf{D}_{\boldsymbol{\theta}_\mathbf{m}}$ contains the motor moments of inertia which are too small compared with the moments of inertia of the spacecraft and manipulator links containing in inertia-type matrix ${}^\mathbf{0}\mathbf{D}_\mathbf{q}^*$. Thus, the controller achieves both the desired manipulator configuration and end-effector position.

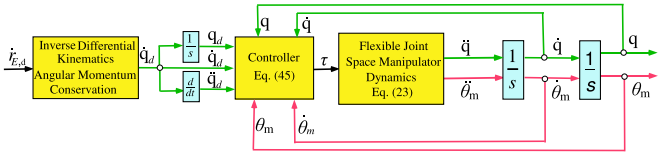

Fig. 11. The block diagram of the proposed closed-loop system.

Although the proposed controller can drive the end-effector through the desired path, one should examine whether the internal dynamics will be stable also, i.e., whether the internal states will remain bounded. In this case, we control only the link angular position $\mathbf{q}$ and the gear reduction angular position $\boldsymbol{\theta}_\mathbf{m}$ is uncontrolled. The internal dynamics for the free-floating manipulator is

$$\mathbf{H_{qq}}(\mathbf{q})\ddot{\mathbf{q}} + \mathbf{H_{q\theta_m}}(\mathbf{q})\ddot{\boldsymbol{\theta}}_\mathbf{m} + \mathbf{h_1}(\Theta, \dot{\Theta}) = \mathbf{0} \tag{25a}$$

Since the study of internal dynamics is complex, one could study the zero-dynamics in order to make some conclusions about the stability of the internal dynamics. The zero-dynamics result by setting $\mathbf{q} = \dot{\mathbf{q}} = \ddot{\mathbf{q}} = \mathbf{0}$. Thus

$$\ddot{\boldsymbol{\theta}}_\mathbf{m} = -\mathbf{H}_{\mathbf{q}\boldsymbol{\theta}_\mathbf{m}}^{*-1}\mathbf{h}_\mathbf{1}^*(\boldsymbol{\theta}_\mathbf{m}, \dot{\boldsymbol{\theta}}_\mathbf{m}) \tag{49}$$

Note that the controller reference input is the desired manipulator configuration. In case it is desired the end-effector to follow a desired path, the computation of this configuration is feasible only if dynamic singularities are avoided. Thus, the desired end-effector path should lie in the PIW area of the manipulator workspace (Papadopoulos & Dubowsky, 1993; Nanos & Papadopoulos, 2011), or else the spacecraft initial attitude should be inside a feasible range (Nanos & Papadopoulos, 2012).

Fig. 11 shows the block diagram of the proposed closed-loop system. The end-effector motion is defined by the end-effector desired velocity $\dot{\mathbf{r}}_{\mathbf{E,d}}$, as shown in Fig. 11. The desired joint rates $\dot{\mathbf{q}}_\mathbf{d}$ are provided by the inverse differential kinematics and the angular momentum conservation (Nanos & Papadopoulos, 2012).

Example 2**:** To illustrate the developed method, the planar 7-dof space manipulator system with parameters in Tables 1 and 2 is employed. The desired path of the end-effector is a circle with centre the point (11.5, 6.5) m and radius R=1.5 m. The static

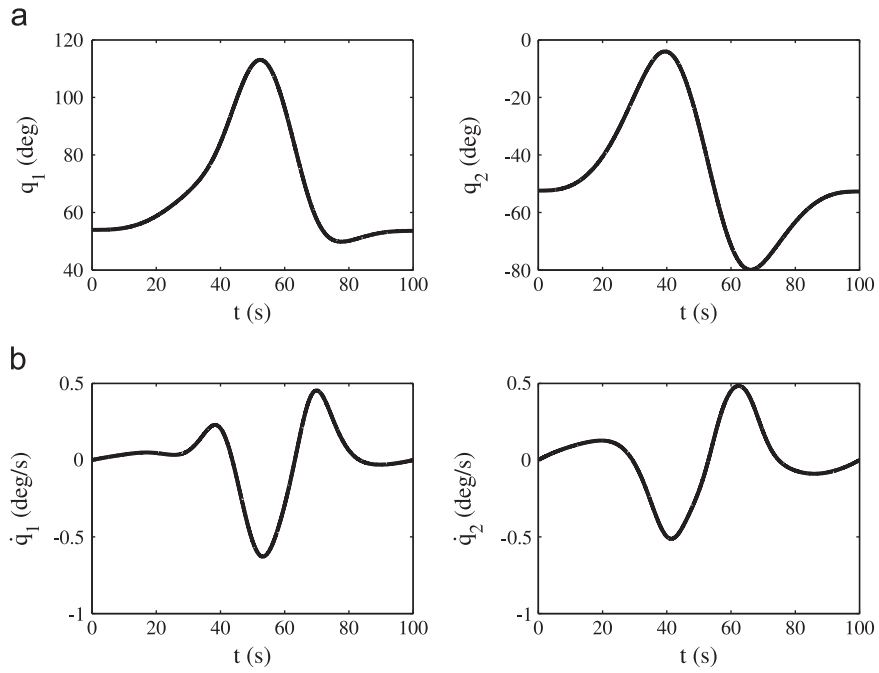

Fig. 12. (a) Trajectories of the manipulator relative joint angles, (b) rates of manipulator relative joint angles.

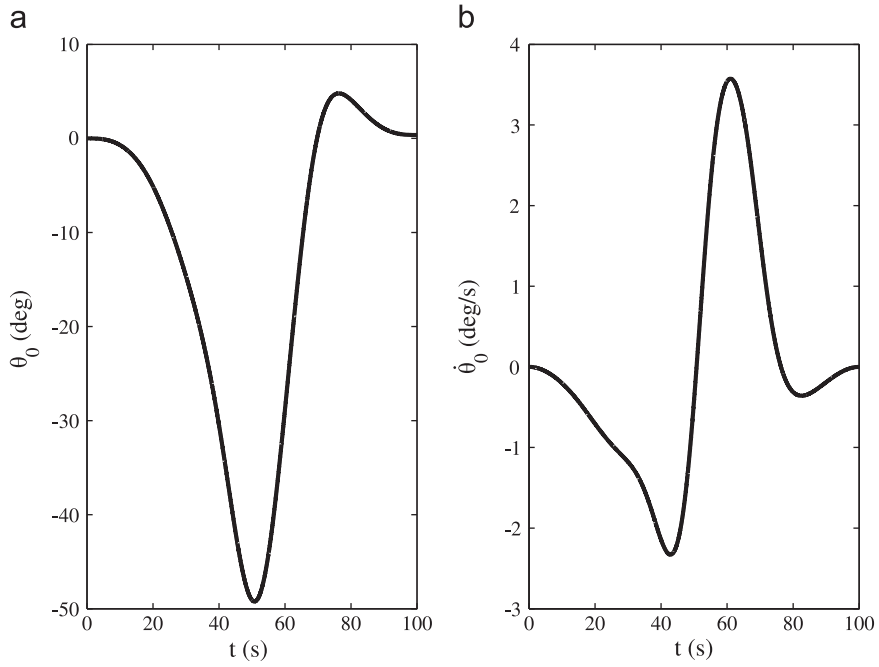

Fig. 13. (a) Trajectory of spacecraft attitude, (b) spacecraft angular velocity.

feedback control law, given by (45), is applied. The selected gain matrices are

$$\mathbf{K_P} = \begin{bmatrix} 0.11 & 0 \\ 0 & 0.11 \end{bmatrix}, \quad \mathbf{K_D} = \begin{bmatrix} 0.7 & 0 \\ 0 & 0.7 \end{bmatrix}, \quad \mathbf{K_I} = \begin{bmatrix} 0.05 & 0 \\ 0 & 0.05 \end{bmatrix} \tag{50}$$

It can be shown that the desired path belongs in the PDW area of the reachable workspace of the manipulator (Papadopoulos & Dubowsky, 1993; Nanos & Papadopoulos, 2011, 2012). Therefore, first one should guarantee that any possible Dynamic Singularity (DS) during the end-effector motion will be avoided. As it has been shown (Nanos & Papadopoulos, 2012), the DS avoidance is feasible if the spacecraft initial attitude belongs in an appropriate range. For the above desired path, the spacecraft initial attitude $\theta_{0,in} = 0°$ ensures DS avoidance.

Fig. 12 shows the trajectories of the manipulator relative angles and their corresponding rates. Fig. 13 shows the spacecraft angular velocity and attitude resulting by the angular momentum conservation. Fig. 14 shows the uncontrolled gear reduction angular positions and velocities and Fig. 15 shows the joint torques applied by the motors so that the end- effector follows the desired path. Finally, the motion of the end-effector and the corresponding motion of the free-floating space manipulator is shown in Fig. 16.

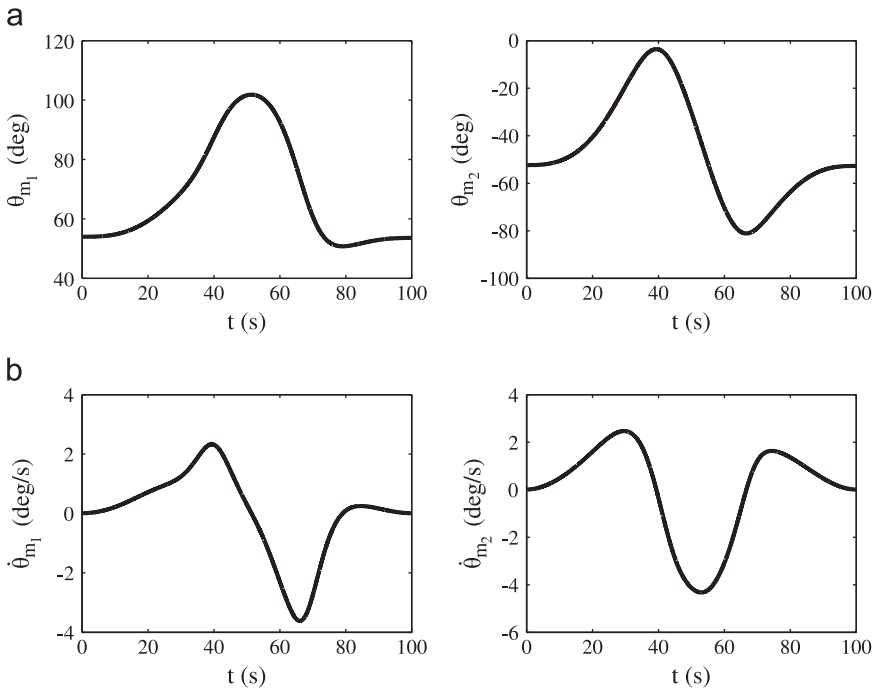

Fig. 14. (a) Trajectories of gear reduction angles, (b) rates of gear reduction angles.

As can be seen from Fig. 16, the applied controller achieves accurate end-effector tracking although only the manipulator configuration is controlled.

5. Conclusions

In this paper, we studied the dynamics of space manipulators, considering that all flexibilities are lumped at the joints.Using the Lagrange approach, the dynamic model was obtained where the link and motor equations are dynamically coupled both through the elastic torque at the joints and at the acceleration level. It was shown that the structure of the dynamics of the flexible joint space manipulators differs than the model structure of the terrestrial ones. The derived model structure gives new opportunities in the design of trajectory following controllers. Therefore, exploiting the structure of the derived dynamic model, the system can be linearized and decoupled via a static feedback linearization controller whose computational effort is feasible in space applications. It was shown that the proposed controller can be applied also in Cartesian space so that the end-effector follows a desired path in the presence of joint flexibilities maintaining a desirable non-oscillatory motion of the spacecraft. The application of the method was illustrated by an example.

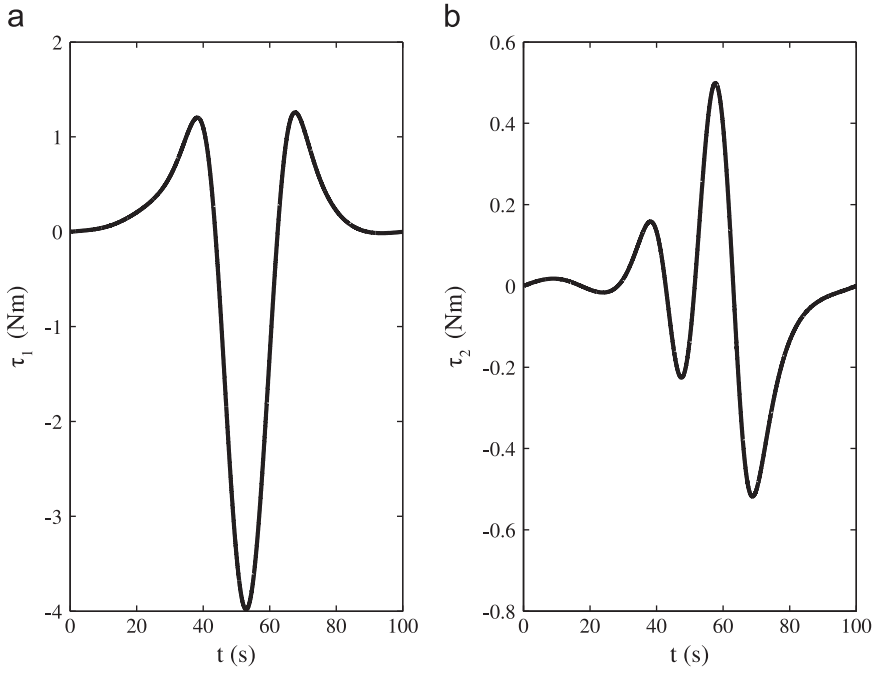

Fig. 15. The motor torques required for following the desired path.

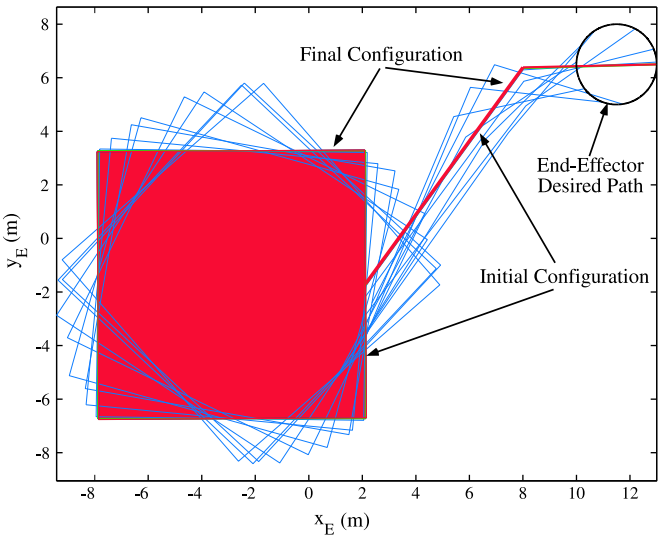

Fig. 16. Motion animation of the space manipulator motion.

Appendix A

The inertia matrix ${}^{\mathbf{0}}\mathbf{D}_{\boldsymbol{\theta}\mathbf{m}}$ in (9a) is given by

$${}^{\mathbf{0}}\mathbf{D}_{\boldsymbol{\theta}\mathbf{m}} = [n_1 {}^{\mathbf{0}}\mathbf{R}_{\mathbf{m_1}} \cdot {}^{\mathbf{m_1}}\mathbf{I}_{\mathbf{m_1}} \cdot {}^{\mathbf{m_1}}\mathbf{z}_{\mathbf{m_1}} \ \cdots \ n_N {}^{\mathbf{0}}\mathbf{R}_{\mathbf{m_N}} \cdot {}^{\mathbf{m_N}}\mathbf{I}_{\mathbf{m_N}} \cdot {}^{\mathbf{m_N}}\mathbf{z}_{\mathbf{m_N}}] \tag{A1}$$

where n_i is the gear ratio of motor i, ${}^{\mathbf{0}}\mathbf{R}_{\mathbf{m}_i}$ is the rotation matrix between the motor i frame $\{m_i\}$ and the spacecraft frame $\{0\}$. The matrix ${}^{\mathbf{m}_i}\mathbf{I}_{\mathbf{m}_i}$ is the motor i inertia tensor relative to its principal axes, expressed in the frame $\{m_i\}$ and the vector ${}^{\mathbf{m}_i}\mathbf{z}_{\mathbf{m}_i}$ is the unit vector in the direction of the motor i rotation axis, expressed in the frame $\{m_i\}$.

The inertia matrix ${}^{\mathbf{0}}\mathbf{D}_{\mathbf{q}\boldsymbol{\theta}\mathbf{m}}$ in (13b) is given below

$${}^{\mathbf{0}}\mathbf{D}_{\mathbf{q}\boldsymbol{\theta}\mathbf{m}} = [n_1 {}^{\mathbf{0}}\mathbf{J}_{22,0}^T \cdot {}^{\mathbf{0}}\mathbf{I}_{\mathbf{m_1}} \cdot {}^{\mathbf{0}}\mathbf{z}_{\mathbf{m_1}} \ \cdots \ n_N {}^{\mathbf{0}}\mathbf{J}_{22,\mathbf{N}}^T \cdot {}^{\mathbf{0}}\mathbf{I}_{\mathbf{m_N}} \cdot {}^{\mathbf{0}}\mathbf{z}_{\mathbf{m_N}}] \tag{A2}$$

where ${}^{\mathbf{0}}\mathbf{I}_{\mathbf{m}_i}$ is the motor i inertia tensor relative to its principal axes, expressed in the frame $\{0\}$ and the vector ${}^{\mathbf{0}}\mathbf{z}_{\mathbf{m}_i}$ is the unit vector in the direction of the motor i rotation axis, expressed in the frame $\{0\}$ and

$${}^{\mathbf{0}}\mathbf{J}_{22,\mathbf{k}} \equiv \left[{}^{\mathbf{0}}\mathbf{z}_{\mathbf{1}} \ \cdots \ {}^{\mathbf{0}}\mathbf{z}_{\mathbf{k}} \ \ \mathbf{0}_{\mathbf{3\times(N-k)}} \right] \tag{A3}$$

where ${}^{\mathbf{0}}\mathbf{z}_{\mathbf{i}}$is the unit vector in the direction of the joint i rotation axis, expressed in the frame $\{0\}$.

The inertia matrix $\mathbf{D}_{\boldsymbol{\theta}\mathbf{m}\boldsymbol{\theta}\mathbf{m}}$ in (13c) is

$$\mathbf{D}_{\boldsymbol{\theta}\mathbf{m}\boldsymbol{\theta}\mathbf{m}} = \begin{bmatrix} n_1^2 I_{m1} & 0 & \cdots & 0 \\ 0 & n_2^2 I_{m2} & 0 & \vdots \\ \vdots & \vdots & \ddots & 0 \\ 0 & \cdots & 0 & n_N^2 I_{mN} \end{bmatrix} \tag{A4}$$

where I_{m2} is the moment inertia of motor i relative to the motor i rotation axis.

Appendix B

Here, the inertia type matrices and the column vector of centrifugal and Coriolis forces presented in (27), for the planar 7-dof manipulator shown in Fig. 4, are given.

The inertia type matrix ${}^0D^*$ is

$${}^0D^* = {}^0D_0^* + {}^0D_1^* + {}^0D_2^* \tag{B1}$$

where

$${}^0D_0^* = d_{00}^* + d_{10}^* + d_{20}^* \tag{B2.1}$$

$${}^0D_1^* = d_{01}^* + d_{11}^* + d_{21}^* \tag{B2.2}$$

$${}^0D_2^* = d_{02}^* + d_{12}^* + d_{22}^* \tag{B2.3}$$

and

$$d_{00}^* = a_{00}^* \tag{B3.1}$$

$$d_{10}^* = a_{10}^* \cos(q_1) \tag{B3.2}$$

$$d_{20}^* = a_{20}^* \cos(q_1 + q_2) \tag{B3.3}$$

$$d_{11}^* = a_{11}^* \tag{B3.4}$$

$$d_{21}^* = a_{21}^* \cos(q_2) \tag{B3.5}$$

where

$$a_{00}^* = I_0^* + m_0^*(m_1^* + m_2^*)r_0^{*2}/(m_0^* + m_1^* + m_2^*) \tag{B4.1}$$

$$a_{10}^* = m_0^* r_0^*(l_1^*(m_1^* + m_2^*) + r_1^* m_2^*)/(m_0^* + m_1^* + m_2^*) \tag{B4.2}$$

$$a_{20}^* = m_0^* m_2^* r_0^* l_2^*/(m_0^* + m_1^* + m_2^*) \tag{B4.3}$$

$$\alpha_{11}^* = I_1^* + (m_0^* m_1^* l_1^{*2} + m_1^* m_2^* r_1^{*2})/(m_0^* + m_1^* + m_2^*) + m_0^* m_2^*(l_1^* + r_1^*)^2/(m_0^* + m_1^* + m_2^*) \tag{B4.4}$$

$$\alpha_{21}^* = m_2^* l_2^*(m_1^* r_1^* + m_0^*(l_1^* + r_1^*))/(m_0^* + m_1^* + m_2^*) \tag{B4.5}$$

$$\alpha_{22}^* = I_2^* + m_2^*(m_0^* + m_1^*)l_2^{*2}/(m_0^* + m_1^* + m_2^*) \tag{B4.6}$$

Note that the equivalent lengths l_i^*, r_i^* as well as the equivalent masses m_i^* and the moment of inertia I_i^* are computed using (3a) and (3b), and (7a) and (7b), respectively, which for planar systems, take the following form:

$$l_i^* = \frac{m_i}{m_i + m_{mi}} l_i \tag{B5.1}$$

$$r_i^* = r_i + \frac{m_{mi}}{m_i + m_{mi}} l_i \tag{B5.2}$$

and

$$I_i^* = I_i + I_{mi+1} + \frac{m_i m_{mi}}{m_i + m_{mi}} l_i^2 \tag{B5.3}$$

The inertia type matrix ${}^{\mathbf{0}}\boldsymbol{D}_{\boldsymbol{\Theta}}$ is

$${}^{\mathbf{0}}\boldsymbol{D}_{\boldsymbol{\Theta}} = \left[{}^0D_1^* + {}^0D_2^* \ \ {}^0D_2^* \ \ n_1 I_{m1} \ \ n_2 I_{m2} \right] \tag{B6}$$

The inertia type matrix ${}^{\mathbf{0}}\mathbf{D}_{\boldsymbol{\Theta}\boldsymbol{\Theta}}$ is

$${}^{\mathbf{0}}\mathbf{D}_{\boldsymbol{\Theta}\boldsymbol{\Theta}} = \begin{bmatrix} d_{11}^* + 2d_{12}^* + d_{22}^* & d_{12}^* + d_{22}^* & 0 & n_2 I_{m2} \\ d_{12}^* + d_{22}^* & d_{22}^* & 0 & 0 \\ 0 & 0 & n_1^2 I_{m1} & 0 \\ n_2 I_{m2} & 0 & 0 & n_2^2 I_{m2} \end{bmatrix} \tag{B7}$$

The terms $\hat{d}_{ij}^*$ of the vector of centrifugal and Coriolis forces given by (29a) and (29b) are

$$\hat{d}_{01}^{*} = a_{10}^{*} \sin(q_1) \tag{B8.1}$$

$$\hat{d}_{02}^{*} = a_{20}^{*} \sin(q_1 + q_2) \tag{B8.2}$$

$$\hat{d}_{12}^{*} = a_{21}^{*} \sin(q_2) \tag{B8.3}$$

Appendix C

Here, the inertia type matrices $\mathbf{H}_{\mathbf{qq}}^{*}$, $\mathbf{H}_{\mathbf{q\theta m}}$ and $\mathbf{H}_{\mathbf{\theta m \theta m}}$ presented in (24a), for the planar 7-dof manipulator shown in Fig. 4, are given bellow:

$$\mathbf{H}_{\mathbf{qq}}^{*} = \begin{bmatrix} d_{11}^{*} + 2d_{12}^{*} + d_{22}^{*} - \dfrac{({}^{0}D_1^{*} + {}^{0}D_2^{*})^2}{{}^{0}D^{*}} & d_{12}^{*} + d_{22}^{*} - \dfrac{{}^{0}D_2^{*}({}^{0}D_1^{*} + {}^{0}D_2^{*})}{{}^{0}D^{*}} \\ d_{12}^{*} + d_{22}^{*} - \dfrac{{}^{0}D_2^{*}({}^{0}D_1^{*} + {}^{0}D_2^{*})}{{}^{0}D^{*}} & d_{22}^{*} - \dfrac{{}^{0}D_2^{*2}}{{}^{0}D^{*}} \end{bmatrix} \tag{C1}$$

$$\mathbf{H}_{\mathbf{q\theta m}} = \begin{bmatrix} -\dfrac{({}^{0}D_1^{*} + {}^{0}D_2^{*})n_1 I_{m1}}{{}^{0}D^{*}} & n_2 I_{m2} - \dfrac{({}^{0}D_1^{*} + {}^{0}D_2^{*})n_2 I_{m2}}{{}^{0}D^{*}} \\ -\dfrac{{}^{0}D_2^{*} n_1 I_{m1}}{{}^{0}D^{*}} & -\dfrac{{}^{0}D_2^{*} n_2 I_{m2}}{{}^{0}D^{*}} \end{bmatrix} \tag{C2}$$

$$\mathbf{H}_{\mathbf{\theta m \theta m}} = \begin{bmatrix} n_1^2 I_{m1} - \dfrac{n_1^2 I_{m1}^2}{{}^{0}D^{*}} & -\dfrac{n_1 I_{m1} n_2 I_{m2}}{{}^{0}D^{*}} \\ -\dfrac{n_1 I_{m1} n_2 I_{m2}}{{}^{0}D^{*}} & n_2^2 I_{m2} - \dfrac{n_2^2 I_{m2}^2}{{}^{0}D^{*}} \end{bmatrix} \tag{C3}$$

Appendix D

The terms h_{ij} in (33a) are given by

$$h_{11} = I_1 + m_1 l_1^2 + I_2 + m_2((l_1 + r_1)^2 + l_2^2 + 2l_2(l_1 + r_1)\cos(q_2)) + I_{m2} + m_{m2}(l_1 + r_1)^2 \tag{D1}$$

$$h_{12} = I_2 + m_2(l_2(l_1 + r_1)\cos(q_2) + l_2^2) \tag{D2}$$

$$h_{22} = I_2 + m_2 l_2^2 \tag{D3}$$

References

Book, J. W. (1993). Structural flexibility of motion systems in the space environment. *IEEE Transactions on Robotics and Automation*, *9*(5), 524–530.

De Luca, A. (1998). *Trajectory Control of flexible Manipulators, Control Problems in Robotics and Automation, Book Chapter* (pp. 83–104)Springer.

De Luca, A., & Lucibello, P. (1998). A general algorithm for dynamic feedback linearization of robots with elastic joints, In *International Conference on Robotics and Automation (ICRA 98)* (pp. 504–510). Leuven, Belgium.

De Luca, A., Lucibello, Schroder, D., Thummel, M. (2007). An acceleration-based state observer for robot manipulators with elastic joints. In *International Conference on Robotics and Automation (ICRA 07)* (pp. 3817–3823) (April 10–14). Roma, Italy.

Ferretti, G., Magnani, G. A., Rocco P., Viganò, L., & Rusconi, A., (2005). On the use of torque sensors in a space robotics application. In *IEEE/RSJ International Conference on Intelligent Robots and Systems (IROS'05)* (pp. 1947–1952) (August 2–6). Edmonton, Alberta, Canada.

Hung, J.Y., and Spong M. W., (1989). Adaptive control of flexible joint manipulators. In *International Conference on Robotics and Automation (ICRA 89)* (pp. 1188–1193). Scottsdale, AZ.

Hu, Y. R., & Vucovich, G., (1997). Modeling and control of free-flying flexible joint coordinated robots. In *Proceedings of the 8th International Conference on Advanced Robotics* (pp. 1013-1020) (7–9 July).

Lozano, R., Valera, A., Albertos, P., Arimoto, S., & Nakayama, T. (1999). PD control of robot manipulators with joint flexibility, actuators dynamics and friction. *Automatica*, *35*, 1697–1700.

Martin, E., Papadopoulos, E., & Angeles, J., (1999). A novel approach to reduce dynamic interactions in space robots. *In Proceeding of the 1999 IASTED International Conference on Robotics and Applications* (October) Santa Barbara, CA.

Nanos, K., & Papadopoulos, E. (2011). On the use of free-floating space robots in the presence of angular momentum. *Intelligent Service Robotics, Special Issue on Space Robotics*, *4*(1), 3–15.

Nanos, K., & Papadopoulos, E., (2012), On Cartesian motions with singularity avoidance for free-floating space robots. In *International Conference on Robotics and Automation (ICRA 12)* (pp. 5398–5540) (May 14–18). St. Paul, MN, USA, .

Papadopoulos, E., & Dubowsky, S. (1993). Dynamic Singularities in Free-Floating Space Manipulators. *ASME Journal of Dynamic Systems, Measurement and Control*, *115*(1), 44–52.

Spong, M. W. (1987). Modeling and control of elastic joint robots,. *ASME Journal of Dynamic Systems, Measurement, and Control*, *109*, 310–319.

Tomei, P. (1991). A simple PD controller for robots with elastic joints. *IEEE Transactions on Automatic Control*, *36*, 1208–1213.

Ulrich, S., & Sasiadek, J. Z. (2012). Modeling and direct adaptive control of a flexible-joint manipulator. *Journal of Guidance and Control, and Dynamics*, *35*(1), 25–39.